Article

Inter-Comparison of Gauge-Corrected Global Satellite Rainfall Estimates and Their Applicability for Effective Water Resource Management in a Transboundary River Basin: The Case of the Meghna River Basin

Islam M. Khairul [1,2,*], Nikolaos Mastrantonas [3,4], Mohamed Rasmy [1,2], Toshio Koike [1,2] and Kuniyoshi Takeuchi [5] [iD]

[1] International Centre for Water Hazard and Risk Management (ICHARM), Public Works Research Institute (PWRI), Tsukuba, Ibaraki 305-8516, Japan; abdul@pwri.go.jp (M.R.); koike@icharm.org (T.K.)
[2] National Graduate Institute for Policy Studies (GRIPS), Tokyo 106-8677, Japan
[3] Centre for Ecology & Hydrology, Maclean Building, Wallingford, Oxfordshire OX10 8BB, UK; nikmas@ceh.ac.uk
[4] IHE Delft, 2601 DA, Delft, The Netherlands
[5] University of Yamanashi, Takeda, Kofu, Yamanashi 400-8510, Japan; takeuchi@yamanashi.ac.jp
[*] Correspondence: k-islam55@pwri.go.jp or kl96wre@gmail.com; Tel.: +81-29-879-6809

Abstract: The Meghna River basin is a transboundary basin that lies in Bangladesh (~40%) and India (~60%). Due to its terrain structure, the Bangladesh portion of the basin experiences frequent floods that cause severe human and economic losses. Bangladesh, as the downstream nation in the basin, faces challenges in receiving hydro-meteorological and water use data from India for effective water resource management. To address such issue, satellite rainfall products are recognized as an alternative. However, they are affected by biases and, thus, must be calibrated and verified using ground observations. This research compares the performance of four widely available gauge-adjusted satellite rainfall products (GSRPs) against ground rainfall observations in the Meghna basin within Bangladesh. Further biases in the GSRPs are then identified. The GSRPs have both similarities and differences in terms of producing biases. To maximize the usage of the GSRPs and to further improve their accuracy, several bias correction and merging techniques are applied to correct them. Correction factors and merging weights are calculated at the local gauge stations and are spatially distributed by adopting an interpolation method to improve the GSRPs, both inside and outside Bangladesh. Of the four bias correction methods, modified linear correction (MLC) has performed better, and partially removed the GSRPs' systematic biases. In addition, of the three merging techniques, inverse error-variance weighting (IEVW) has provided better results than the individual GSRPs and removed significantly more biases than the MLC correction method for three of the five validation stations, whereas the two other stations that experienced heavy rainfall events, showed better results for the MLC method. Hence, the combined use of IEVW merging and MLC correction is explored. The combined method has provided the best results, thus creating an improved dataset. The applicability of this dataset is then investigated using a hydrological model to simulated streamflows at two critical locations. The results show that the dataset reproduces the hydrological responses of the basin well, as compared with the observed streamflows. Together, these results indicate that the improved dataset can overcome the limitations of poor data availability in the basin and can serve as a reference rainfall dataset for wide range of applications (e.g., flood modelling and forecasting, irrigation planning, damage and risk assessment, and climate change adaptation planning). In addition, the proposed methodology of creating a reference rainfall dataset based on the GSRPs could also be applicable to other poorly-gauged and inaccessible transboundary river

basins, thus providing reliable rainfall information and effective water resource management for sustainable development.

1. Introduction

Bangladesh is among the most flood-prone countries in the world, as it is located at the confluence of three of the world's major alluvial rivers, the Ganges, Brahmaputra, and Meghna (GBM) [1]. Due to the combined influence of these transboundary rivers, frequent floods cause devastating fatalities and socio-economic damage in the country every year [2,3]. The Meghna basin experiences particularly heavy damage due to its complex terrain structure, abundant precipitation originating from the world's wettest places (which are within the catchment), and the prolonged duration of flooding due to flow obstructions (either from the combined flow of the Ganges and the Brahmaputra, or from the back-water effect caused by tidal influence) [3–6]. This damage mainly involves loss of life and economic losses because the Bangladesh portion of the basin is home to agriculture and aquaculture activities that support the country's economy and population. The area contributes to rice production during the dry season and provides ample fish during the wet season. Land development in this area has been aggressive over the last two decades and, as a result, the area contributes more than 16% of the country's total rice production [7]. Therefore, water resource management in the basin (e.g., prevention and management of floods and droughts, agricultural management, and water-quality control) is among the nation's top priorities for ensuring food security.

To ensure sound plans for effective water resource management in the Meghna basin, that region's water resources need to be quantified, and predictive information (e.g., flood and drought forecasting) needs to be generated. Doing so will require hydrological modelling, which further requires accurate estimation of precipitation, which is a primary driving force of such models [8,9]. However, hydrological modelling and forecasting are very difficult to perform in this basin because the majority of the catchment area (~60%) is located in India and because India and Bangladesh do not share hydro-meteorological (rainfall, streamflow, river water level, etc.) and water-use (irrigation, storage, etc.) data [3,10–12]. In addition, ground-based rainfall measurements inside Bangladesh are sparse in both time and space. All this contributes to the lack of basin-wide hydro-meteorological data, both real-time and historical, which has caused water resource management in this basin to be extremely challenging for Bangladesh, resulting in massive socio-economic damage to the nation.

Fortunately, in recent years, many satellite-based rainfall estimates with high spatial and temporal resolutions have been generated at the global scale and have become available at no cost and in near-real time (NRT). These globally-available NRT satellite-based rainfall products include Global Satellite Mapping of Precipitation (GSMaP) from the Japan Aerospace Exploration Agency (JAXA), Tropical Rainfall Measuring Mission (TRMM) Multi-satellite Precipitation Analysis (TMPA) from the National Aeronautics and Space Administration (NASA), Integrated Multi-satellitE Retrievals for GPM (IMERG) from NASA, the Climate Prediction Centre (CPC) MORPHing method (CMORPH) from the National Oceanic and Atmospheric Administration (NOAA), and Precipitation Estimation from Remotely Sensed Information using Artificial Neural Networks (PERSIANN) from the University of California, Irvine. These sets of satellite-based information are highly valuable and have immense potential in water resource management, particularly for inaccessible transboundary and poorly-gauged river basins. Given the absence of upstream rainfall data from India's portion of the Meghna basin, satellite data (which includes rainfall estimates for both inside and outside Bangladesh) can overcome the limitations of poor data availability and can also be used as gridded

reference data to generate basin-wide hydrological responses of the basin or to practice effective and timely management of water resources and water-related disasters.

However, satellite data come with the caveat that they must be verified with ground observations prior to their application, as such data are subject to systematic and random errors because they rely on indirect estimation from radiances; because of issues with their sampling frequency and rainfall-retrieval algorithms; and because they depend on elevation, latitude, rainfall type, and climate [13–19]. Therefore, many NRT satellite products have recently been supplemented with gauge adjustments based on global gauge observations, both for research purposes and for use in a wide range of applications. They are available at no cost, usually 10–20 days after the end of each month. The most important of these products are the Climate Hazards Group InfraRed Precipitation with Station data (CHIRPS), adjusted GSMaP (GSMaP_Gauge); TRMM 3B42 (three-hourly or daily) and 3B43 (monthly) Version 5 (V5), Version 6 (V6), and Version 7 (V7); corrected CMORPH Version 1 (CMORPH_ V1.0_CRT) and blended CMORPH Version 1 (CMORPH_ V1.0_BLD); adjusted PERSIANN (PERSIANN-CDR); and Multi-Source Weighted-Ensemble Precipitation (MSWEP). Some of these gauge-adjusted products include in situ measurements for the Meghna basin as well, both inside and outside Bangladesh, so they may have greater potential than the NRT products for use as a reference rainfall dataset for long-term hydrological applications in the basin. However, before these products can be used, further bias correction may be necessary, as the global validation stations (provided by NASA, NOAA, JAXA, CPC, and many other global databases) are limited and usually far away and, thus, may not sufficiently represent the actual rainfall characteristics of the basin. Another reason could be that bias originates from various correction algorithms and methods. For instance, (1) the CHIRPS algorithm uses satellite imagery with the available time series of global station data for a month, producing daily CHIRPS data in the third week of the following month; (2) the adjusted GSMaP product combines standard and re-analysis based satellite estimates with 0.5°-grid CPC global gauge analysis (CPC grid box contains the average rainfall of the available gauges located within that box); and (3) the corrected daily TRMM 3B42 is a disaggregated product from corrected monthly TRMM 3B43 that is produced by calibrating monthly TRMM 3B42RT estimates (NRT version) with the monthly Global Precipitation Climatological Center's (GPCC) and CPC's rain-gauge analysis. Missing rainfall records and the limited number of such records in the global database may also affect the accuracy of these gauge-adjusted satellite products demanding further bias correction.

Several studies have been conducted on the Bangladesh portion of the GBM basins, using both NRT and gauge-adjusted, satellite-based rainfall products. In an effort to understand the climatic characteristics of rainfall in Bangladesh, Islam and Uyeda [20] depicted that TRMM 3B42 (V6), without further correction, overestimated the rainfall in the pre-monsoon period and underestimated it in the monsoon period; they also found that the biases were mainly seasonal- and location-dependent. Blended with concurrent ground observations wherever available, Nishat and Rahman [21] used TRMM 3B42 (V6) satellite data to model the GBM basins for streamflow prediction. In their study, the monthly flow volume simulated with a lumped kind (sub-basin scale) of model differed from the actual streamflows in all three basins, which suggested that their GBM model forced with satellite data has limited potential for water resource management. Valeriano et al. [22] attempted to generate discharge in the Meghna basin using TRMM 3B42 (V6) estimates. They further improved the satellite data using two approaches: by applying a simple ratio-correction method at the available local gauge stations and then transferring the correction factors to other grids (according to Thiessen polygon areas of influence) inside Bangladesh, and by applying the nearest-neighbour method to the area outside Bangladesh. Rather than a daily time-series comparison, their study involved a comparison of the total discharge for the rainy season throughout 2001–2004 with the observed discharge from the same period. To learn the causes of the 2007 Bangladesh flood, Islam et al. [23] compared the mean monthly rainfall, as calculated from 3-hourly TRMM-3B42 (V6) estimates (without further corrections), with that of the historical rainfall for the flood period. They found that a larger volume of rainfall was accumulated in July 2007 than in the same month in either of the previous two years, causing flooding in Bangladesh. Over the

domain of the GBM basins, Prasanna et al. [24] developed a merged rainfall dataset (0.5° resolution) for 1998–2007 using TRMM-3B42 (V6) estimates and gauge rainfall data collected from India and Bangladesh; they consequently predicted the possibility of using this dataset for flood forecasting. However, no hydrological models were either calibrated or validated in their study so as to check the streamflow generation; such a step is desirable for flood forecasting. Siddique-E-Akbor et al. [25] ran a distributed hydrological model forced with datasets from two NRT satellite-precipitation products (TRMM-3B42RT and CMORPH) to investigate the feasibility of water management in the GBM basins. However, they mainly focused on hydrological simulation of the Brahmaputra and Ganges basins and did not provide any bias correction of the NRT satellite products.

None of the researchers in those previous studies—even though they hinted at the promise of using satellite-based rainfall products in hydrological studies of data-scarce river basins, such as the Meghna basin—assessed different satellite-based rainfall products to investigate their potential for use as reference dataset in simulating hydrological responses of a basin for water resource management. Therefore, this study is focused on evaluating the performance of four gauge-adjusted satellite rainfall products (GSRPs): CHIRPS, GSMaP_Gauge (termed GSMaP-G), TRMM-3B42 Version 7 (termed TMPA-G), and MSWEP, during 2009–2016. This study also identifies the biases of the GSRPs relative to the ground rainfall measurements for the area inside Bangladesh, and it applies several bias-correction and merging techniques to further remove biases from the GSRPs. The bias-correction and merging techniques are conducted at the available gauge stations inside Bangladesh to calculate correction factors and merging weights, respectively. These station-based correction factors and merging weights are spatially distributed using the inverse distance weighting (IDW) interpolation method [26–28] to produce grid-based correction-factor and merging-weight maps that cover the entire Meghna basin. The original GSRPs are then multiplied or added to these factor maps (multiplication or addition is dependent on the bias-correction and merging techniques), resulting in improved (bias-corrected or merged) satellite datasets. The study further investigates the improved dataset's potential for use as a reference rainfall data for streamflow simulations of the Meghna basin.

This study therefore has three key objectives: (1) to evaluate the performance of the GSRPs relative to the available ground rainfall measurements in the Bangladesh portion of the Meghna basin; (2) to further improve the GSRPs' rainfall estimates by applying several bias-correction and merging techniques, thus creating an improved rainfall dataset; and (3) to investigate the applicability of the improved dataset as a reference rainfall data in simulating streamflows for water resource management in the basin. The paper is organized as follows: Section 2 introduces the study area; Section 3 presents the various datasets used in this study; the methods are described in Section 4, and Section 5 outlines the results and discusses the findings; and, finally, concluding remarks are presented in Section 6.

2. Study Area

The Meghna (Upper Meghna) basin is a transboundary river basin and shares the area between Bangladesh and India (Figure 1a). It originates in the hills of Manipur and Meghalaya States in India. About 40% of the basin area falls within Bangladesh, and the remaining 60% lies in Indian territory. Specifically, the basin encompasses the mountainous Meghalaya, Assam, Manipur, Tripura, and Mizoram regions of India and the predominantly agricultural land of Bangladesh (22.75–26.00°N, 89.50–94.50°E) (Figure 1a,c,d). The topography of the basin changes rapidly in its northern and eastern areas, and the altitude varies from 1 to 2888 m with a mean of 362 m a.s.l. [29] (Figure 1c). The central part of the basin comprises plains and gentle hills and is, thus, highly vulnerable to flooding. The Barak River, which is the prime source of the Meghna River, bifurcates into the Surma and the Kushiyara Rivers at Amalshid, which is in Sylhet District near the Bangladesh-India border (Figure 1a). Discharges from the steep and highly flashy rivers originating in the Khasi and Jaintia Hills—which are the wettest places in the world, with an annual average rainfall of about 12,000 mm [4,30]—contribute to the Surma River through its right bank. On the other hand, the Kushiyara River receives water from the rivers that originate in the Tripura Hills (e.g., the Manu River). Between

the Surma and Kushiyara rivers are many lowland regions, internal draining depressions (called *Haors*), meandering flood channels, and abandoned river courses, all of which are flooded in every pre-monsoon (flash-flood period) and monsoon season. The channels of the main rivers (e.g., the Surma, Kushiyara, Lubachara, and Jadukata), along with those of many other rivers in the basin, run from the northeast to the southwest and flow through the Bhairab Bazar stream gauge station as the Upper Meghna to join the Padma at Chandpur, and finally flows into the Bay of Bengal as the Lower Meghna (Figure 1a,b). The drainage area of the Upper Meghna is about 76,000 km^2; about 62% of this area comprises forested, mountainous (or hilly) terrain, whereas 29% comprises irrigated cropland and pastures [31] (Figure 1d).

The basin is delineated for streamflow simulation based on HydroSHEDS (Hydrological data and maps based on SHuttle Elevation Derivatives at multiple Scales [29]), considering the outlet at Bhairab Bazar station (Figure 1b). This station is selected for two main reasons; the total flow of the basin is higher at this station, and the streamflow for the entire basin is also measured there. The climatic year in the basin can be divided into wet and dry seasons. Given the rainfall intensity and monthly accumulated rainfall, this study defines March through October as the wet season and November through February as the dry season.
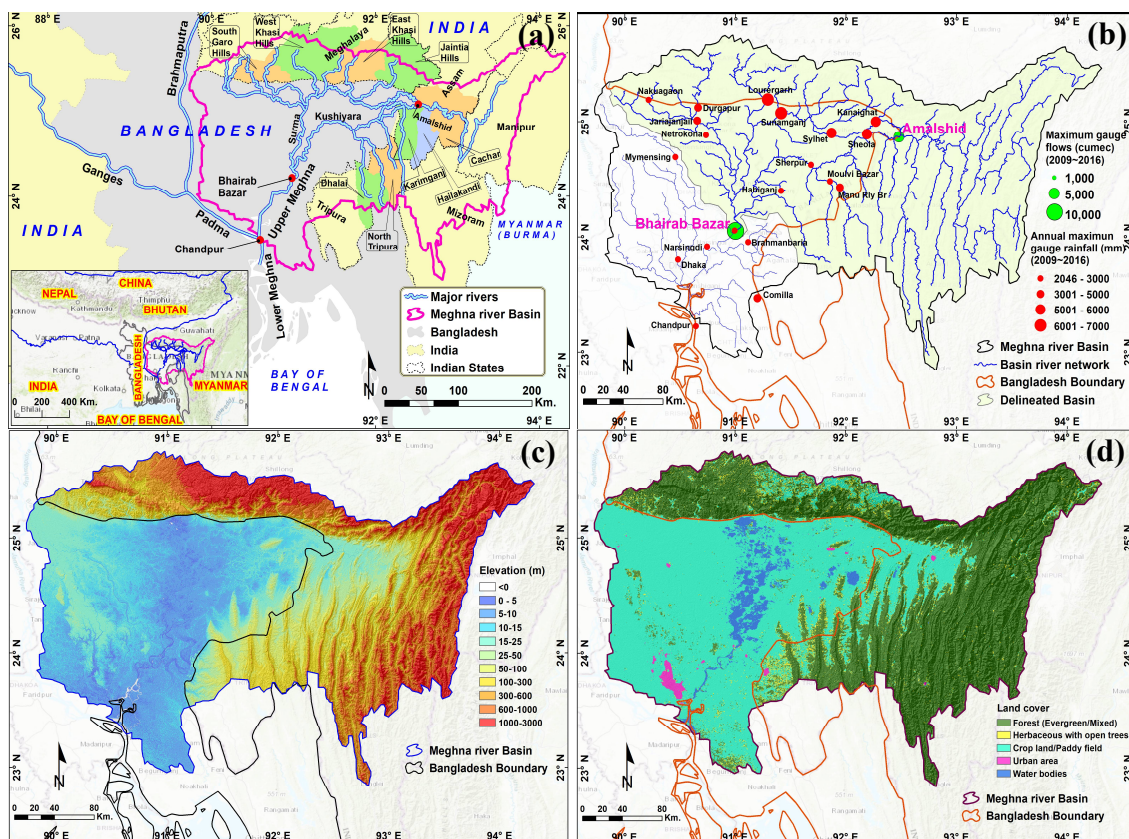

Figure 1. Topographic features of the study area. (**a**) The Meghna basin in the Asian continent (inset), showing major rivers and administrative details; (**b**) the Meghna basin with its detailed river network, including 20 rain-gauge stations (red bubbles) and two streamflow stations (green bubbles) in Bangladesh; (**c**) the HydroSHEDS (90 m resolution) digital elevation model of the Meghna basin; and (**d**) the land cover in the Meghna basin.

3. Data

3.1. Topographic Data

Topographic data are required to set up hydrological models. These data include digital elevation models, river networks, drainage basins, flow directions, and flow accumulation, and they are collected from the U.S. Geological Survey's HydroSHEDS. The HydroSHEDS [29] data are produced using NASA's Shuttle Radar Topography Mission [32] and are in a consistent format for regional- and global-scale applications. These data are freely available at 3-, 15-, and 30-s resolutions.

3.2. Hydro-Meteorological Data

3.2.1. Rainfall

As discussed, Bangladesh does not receive any observed rainfall data for beyond its borders, and the available data are only from inside the country. Out of all the in situ stations maintained by the Bangladesh Water Development Board, 20 are sparsely located within the Bangladesh portion of the Meghna basin. Table 1 outlines the statistics for these 20 rain-gauge stations for the study period (2009–2016), and Figure 1b shows the locations of these stations (red bubbles).

The percentages of the daily rainfall records that are missing in the study period vary from 1.03% to 43.70% for the rain gauge stations (Table 1). Due to the fact that some of the daily data are missing, because the rain gauge network is sparse and only inside Bangladesh, and the fact that gauge records are merely point measurements, it is desirable to have a dense network of rainfall estimates that covers the entire Meghna basin, so as to simulate its hydrological responses, as also recommended by Romilly and Gebremicheal [33]. Given this, this study investigates rainfall estimates of four GSRPs (CHIRPS, GSMaP-G, TMPA-G, and MSWEP) that contain global gauge information for the basin, both inside and outside Bangladesh. The study includes the products that are freely available in near-present time (usually 10–20 days after the end of each month) and that have as high a spatial resolution as possible. The details on each GSRP are as follows.

Table 1. Salient features of the 20 rain-gauge stations located in the Bangladesh portion of the Meghna basin for the study period of 2009–2016. See Figure 1b for a spatial reference.

Sl.	Rain-Gauge Station Name	North Latitude (°)	East Longitude (°)	Elevation (m a.s.l.) (90 m SRTM)	Available Daily Records	Missing Daily Data (%)	Mean Annual Rainfall (mm)
1	Lourergarh	25.1941	91.2941	16	2892	1.03	5130
2	Sunamganj	25.0760	91.4147	14	2875	1.61	5015
3	Sylhet	24.8764	91.8571	20	2922	0.00	4156
4	Kanaighat	25.0011	92.2708	23	2844	2.67	3926
5	Sheola	24.8922	92.1910	20	2447	16.26	3536
6	Durgapur	25.1227	90.6645	20	2152	26.35	2926
7	Netrokona	24.8832	90.7356	14	2842	2.74	2333
8	Habiganj	24.4036	91.4151	11	2692	7.87	2320
9	Comilla	23.4705	91.2000	17	2922	0.00	2312
10	Nakuagaon	25.1900	90.2180	31	2228	23.75	2211
11	Manu RlyBr	24.4324	91.9462	19	1762	39.70	2137
12	Sherpur-Sylhet	24.6277	91.6848	18	1645	43.70	2134
13	Jariajanjail	25.0092	90.6557	9	2669	8.66	2070
14	Moulvi Bazar	24.4849	91.8570	19	2712	7.19	1882
15	Narsingdi	23.9159	90.7456	9	2890	1.10	1815
16	Mymensingh	24.6940	90.4594	10	2410	17.52	1807
17	Chandpur	23.2254	90.6440	10	2780	4.86	1802
18	Brahmanbaria	23.9555	91.1177	17	2922	0.00	1752
19	Dhaka	23.7840	90.5278	10	2725	6.74	1609
20	Bhairab Bazar	24.0559	90.9950	8	2922	0.00	1390

CHIRPS has been created in collaboration with scientists at the U.S. Geological Survey Earth Resources Observation and Science Center, and it incorporates 0.05°- and 0.25°-resolution satellite-measured rainfall time series blended with in situ station data. The blending algorithm

uses satellite imagery and station data to produce a preliminary information product with a latency of about two days and a final product with an average latency of about three weeks. The station processing stream used to produce CHIRPS incorporates data from many public data streams and from several private archives, such as the Global Historical Climatology Network's daily (GHCN-D) [34] and monthly archives, the Global Summary of the Day database, and the World Meteorological Organization's Global Telecommunication System. Additional observations come from various national meteorological agencies. The data for 1981 through the near present (after a 1–3 week delay) are freely available with a daily temporal resolution. For more information on CHIRPS, refer to Funk et al. [35,36].

GSMaP, which is produced by JAXA, integrates geostationary infrared data from three satellites (MTSAT, METEOSAT-7/-8, and GOES-11/12) along with passive microwave data from sensors mounted on various low-Earth-orbiting satellites with an infrared-microwave combined algorithm [37–39], a backward-and-forward morphing technique from infrared images [40], and a Kalman filter [41]. The rain types from the TRMM precipitation radar, the melting-layer model, and the scattering algorithm are used in the radiative transfer model calculation to improve the rain/no-rain classification methods [42] over land [43]. The gauge-adjusted GSMaP version, i.e., GSMaP_Gauge (termed GSMaP-G) is used for this study. GSMaP-G is adjusted from the GSMaP_MVK (standard) and GSMaP_RNL (reanalysis) estimates and includes global gauge analysis (CPC Unified Gauge-Based Analysis of Global Daily Precipitation, 0.5°-grid box), as supplied by NOAA. GSMaP_MVK integrates passive microwave radiometer data with infrared radiometer data. It is produced with a Kalman filter model, which refines the precipitation rate propagated based on the atmospheric moving vector derived from two successive infrared images. GSMaP_RNL, on the other hand, is a reanalysis product based on Japanese 55-year reanalysis data (six-hourly, model grid (TL319L60)) as ancillary data to produce a continuous and homogeneous dataset for the past. The adjustment in GSMaP-G is applied only to the estimation over land and the rain rate over the ocean. The rain rate of GSMaP-G is calculated based on optimal theory, which adjusts the GSMaP-G hourly rain rate so that the sum of the 24-h GSMaP-G rain rate remains roughly the same as the gauge measurement for each period. The GSMaP-G data are freely available on the daily temporal scale and with 0.1° spatial resolution. For more information on GSMaP-G, refer to Ushio et al. [41,44].

TRMM-3B42 Version 7 (termed TMPA-G), which has been released by NASA's Goddard Space Flight Center, is a merged product of satellite-based rainfall estimates and gauge data [45]. The algorithm first combines microwave precipitation estimates from multiple low-Earth-orbiting satellites and then calibrates them to both the TRMM Microwave Imager precipitation (TRMM-2A12) and the TRMM Combined Instrument precipitation (TRMM-2B31). These are merged to produce a microwave-only best estimate for every 3 h. The infrared precipitation estimates from multiple geosynchronous satellites are then calibrated to the microwave estimates and used to fill in the regional gaps in the merged microwave field, thus producing a combined satellite-based rainfall estimate for every 3 h [45,46]. These combined satellite estimates are then summed at the monthly scale and recalibrated with monthly rain-gauge analysis from the GPCC [47] and from the CPC's Climate Assessment and Monitoring System monthly rain-gauge analysis [48], thus providing the final satellite-and-gauge merged precipitation estimates. These monthly estimates are then disaggregated to three-hourly and daily estimates to provide TMPA-G data at 0.25° spatial-resolution. The product is updated 10–15 days after the end of each month. For more information on TMPA-G, refer to Huffman et al. [45].

MSWEP takes advantage of the complementary strengths of gauge-, satellite-, and reanalysis-based data to provide reliable precipitation estimates for the entire globe [49]. MSWEP has been validated at a global scale through observations from ~70,000 gauges and through hydrological modelling for ~9000 catchments [50]. Daily gauge observations have been used to determine the merging weights and wet-day biases for the individual precipitation dataset and to improve the rainfall estimates near the gauge stations. The observation database comprises worldwide in situ

measurements compiled from the GHCN-D database [34], the Global Summary of the Day database, and many other public, private data library. MSWEP data are freely available from 1979–2016 with a three-hourly and daily temporal, and 0.1° and 0.5° spatial-resolution. For more information on MSWEP, refer to Beck et al. [49,50]. A brief summary of the GSRPs is presented in Table 2.

Table 2. Salient features of the GSRPs used in the study for the period of 2009–2016.

GSRP Name	Resolution		Coverage		Latency	Main Reference	Data Links
	Spatial	**Temporal**	**Spatial**	**Temporal**			
CHIRPS	0.25°	daily	Global 50°N–S	1981–present	1–3 weeks	[36]	ftp://ftp.chg.ucsb.edu/pub/org/chg/
GSMaP-G	0.1°	daily	Global 60°N–S	2000–present	2–3 days	[44]	http://sharaku.eorc.jaxa.jp/GSMaP/
TMPA-G	0.25°	daily	Global 50°N–S	1998–present	10–15 days	[45]	ftp://trmmopen.nascom.nasa.gov/pub/
MSWEP	0.1°	daily	Global 60°N–S	1979–2016	-	[49]	http://www.gloh2o.org/

Figure 2 shows some of the global gauge stations and CPC grid centres that, along with other observed datasets, were used to produce GSRP rainfall estimates in and around the Meghna basin. The stations and grid centres are shown for the dates of 25 July 2010, and 17 May 2016. The network of stations is collected from the GHCN-D database provided by NOAA (ftp://ftp.ncdc.noaa.gov/), and the grid centres are derived from the CPC's unified 0.5°-grid boxes, which are also provided by NOAA (http://ftp.cpc.ncep.noaa.gov/precip/CPC_UNI_PRCP/). Each CPC box (0.5° × 0.5°) consists of global gauges located within that box; the number differs for each box (and the minimum number can be 0, as shown in the figure). The average rainfall of the gauges inside a CPC box is considered as the rainfall amount for that box. Based on the figure, the number of GHCN-D stations and the number of gauges inside a CPC box vary by the day according to the gauges' availability.
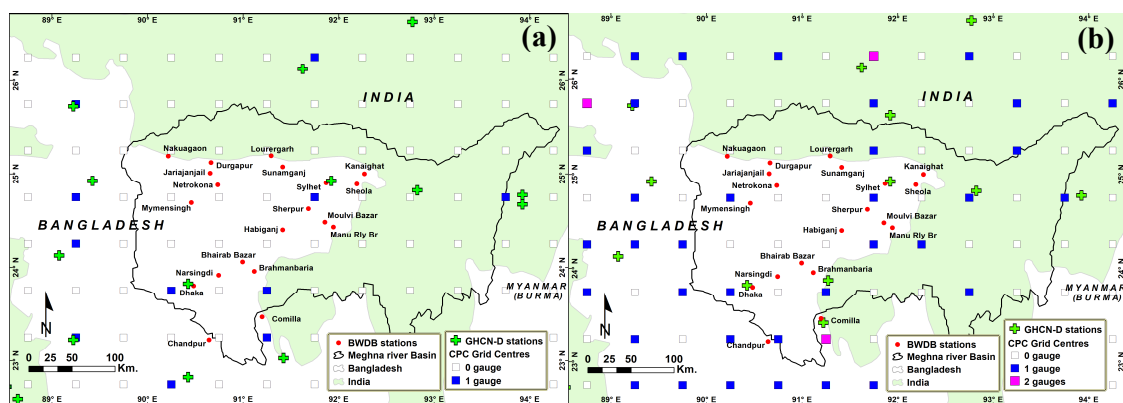

Figure 2. Meghna basin showing the GHCN-D global gauge stations and CPC unified 0.5°-grid centres that—along with other observed datasets—were used to produce the GSRP rainfall estimates on (**a**) 25 July 2010, and (**b**) 17 May 2016. The local 20 Bangladesh Water Development Board's (BWDB) rainfall stations are also presented (red dots).

3.2.2. Water Level and Streamflow

Bangladesh Water Development Board provides observed water level and streamflow data for all hydrological stations located in Bangladesh. While the water-level data are regularly measured five times per day (at 0600, 0900, 1200, 1500, and 1800), the frequency-of-discharge data (measured using the velocity-area method) varies from daily to fortnightly or even monthly. Therefore, in the Meghna basin, rating equations are prepared using observed streamflows and respective water levels

so as to generate daily observed streamflows for the entire study period (2009–2016) at two critical hydrological stations: Bhairab Bazar (located at the outlet of the Meghna basin) and Amalshid (located near the Bangladesh-India border at the Kushiyara River) (Figure 1b, green bubbles).

4. Methods

Figure 3 demonstrates the research method used in this study for the inter-comparison of four GSRPs, the creation of an improved rainfall dataset, and the investigation of that dataset's applicability when simulating hydrological responses for the Meghna basin. First, the performance of the GSRPs is evaluated by comparing them to ground rainfall observations from the local gauges to identify the GSRPs' further biases. Then, a number of bias-correction techniques are applied to re-correct the GSRP estimates. In addition to bias correction, three merging techniques are also investigated to improve the GSRPs' performance. In addition, a combination of merging and bias correction is also explored. Among the bias-corrected and merged products, the product that provides the best results is selected as a reference rainfall dataset. Finally, the applicability of such dataset is investigated to the simulated streamflows using a distributed hydrological model.
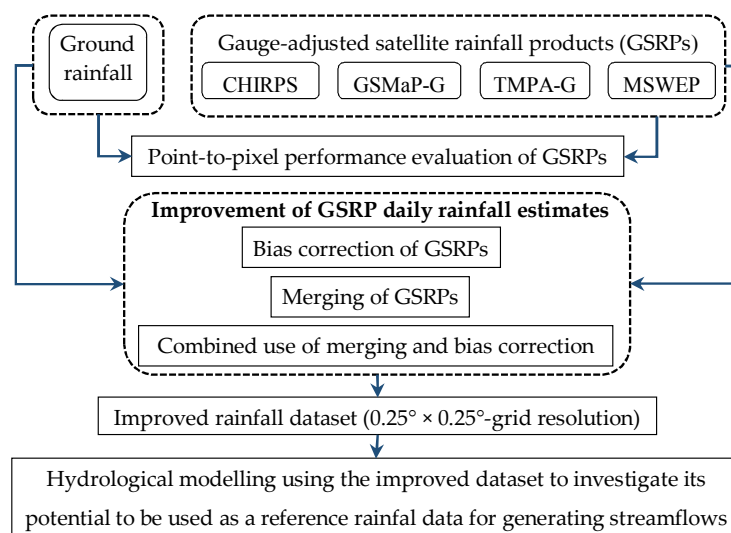

Figure 3. Flow chart of the research structure used in this study for comparing four GSRPs, creating a reference rainfall dataset, and investigating that dataset's applicability when simulating streamflows in the Meghna basin for the purpose of water resource management.

4.1. Performance Evaluation of GSRPs

The daily GSRP rainfall estimates for the wet seasons (March–October) across the entire study period (2009–2016) are validated by comparison with daily ground rainfall records from 20 rain-gauge stations inside Bangladesh on a point-to-pixel basis. The daily pixel data closest to each gauge location are extracted from the GSRPs before performing the comparison. The statistical metrics used for this comparison include normalised-mean-squared error (*NMSE*), relative bias (*RB*), root-mean-squared error (*RMSE*), and correlation coefficient (*CC*). These metrics are defined as follows:

$$NMSE = \frac{1}{N}\sum \frac{\left(P_s - P_g\right)^2}{\frac{1}{N}\sum P_s \, \frac{1}{N}\sum P_g} \tag{1}$$

$$RB = \frac{\sum\left(P_s - P_g\right)}{\sum P_g} \times 100 \tag{2}$$

$$RMSE = \sqrt{\frac{\sum(P_s - P_g)^2}{N}} \tag{3}$$

$$CC = \frac{Cov(P_s P_g)}{\sigma_{P_s} \sigma_{P_g}} \tag{4}$$

where P_s is the rainfall estimate from GSRPs (CHIRPS/GSMaP-G/TMPA-G/MSWEP), P_g is the ground rainfall record, and N is the sample size; Cov and σ in Equation (4) refer to the covariance and the standard deviation, respectively. NMSE is a dimensionless estimator of the overall deviations between P_s and P_g. RB, which measures systematic differences, is measured as a percentage. Accumulated error is measured using RMSE in mm/day for the daily scale, mm/month for the monthly scale, and so on. The agreement between P_s and P_g is measured using CC, which is dimensionless. A perfect validation should have a CC of 1. The lower RMSE, RB, and NMSE, the better the estimation. These comparison indices for validating various satellite-based rainfall products have been used in many prior studies [51–58].

This study uses categorical statistics, such as probability of detection (*POD*), strike ratio (*SR*), false-alarm ratio (*FAR*), and threat score (*TS*), which have been used in many studies [51,56–59], for evaluating the rainfall-detection abilities of the GSRPs relative to the ground rainfall measurements. These statistics are computed using Equations (5)–(8):

$$POD = \frac{\sum A}{\sum(A + B)} \tag{5}$$

$$SR = \frac{\sum(A + D)}{\sum(A + B + C + D)} \tag{6}$$

$$FAR = \frac{\sum C}{\sum(A + C)} \tag{7}$$

$$TS = \frac{\sum A}{\sum(A + B + C)} \tag{8}$$

where A is the number of rainfall events detected both by the gauges and the GSRPs; B and C, respectively, are the number of rainfall events detected by the gauges and the number detected by the GSRPs; and D is the number of non-rainfall events detected both by the gauges and the GSRPs. *POD*, *SR*, *FAR*, and *TS* range from 0 to 1. Perfect detection of rainfall events by the GSRPs relative to the gauges would mean *POD*, *SR*, and *TS* values of 1 and a *FAR* value of 0.

4.2. Bias Correction of GSRPs

Prior to their use for hydrological applications, the GSRPs are further bias-corrected against the ground rainfall measurements to better represent their rainfall estimates for the Meghna basin. Among the many existing bias-correction techniques that have been proposed for correcting satellite data, two widely-used techniques—linear correction and quantile mapping—are implemented and evaluated in this study. In addition, a modified linear correction (MLC) technique is also applied. As with the comparison technique, all of the correction methods are conducted at the available gauge stations inside Bangladesh, and the station-based correction factors are interpolated to each grid cell in the basin for each GSRP (interpolation is performed based on GSRPs' original spatial resolution) to obtain basin-wide corrected rainfall estimates.

4.2.1. Linear Correction Method

This method is applied to correct the GSRPs in a dynamic form, with the correction factors calculated based on two varying time periods (i.e., windows). In the former approach, the correction factors are calculated using mean monthly time window, whereas in the latter approach, a length

of sequential time window across the entire study period is used. The linear correction with mean monthly window (LCMW) technique is very simple and has been used in many studies [18,60–64]. In this technique, the mean monthly correction factors for the 12 calendar months and for each gauge station are calculated in the first step as follows:

$$f_{m,k} = P_{g,m,k} / P_{s,m,k} \tag{9}$$

where $f_{m,k}$ is the correction factor for month m at station k; and where $P_{g,m,k}$ and $P_{s,m,k}$, respectively, are the mean monthly gauge and satellite estimates for month m at station k. In the second step, the spatial distribution of the correction factors from the gauge locations to the grid cells is obtained by adopting the IDW interpolation method [26–28]. Finally, the corrected GSRPs are calculated as follows:

$$P_{scor,m,d\ (i,j)} = f_{m\ (i,j)} * P_{s,m,d\ (i,j)} \tag{10}$$

where $P_{scor,m,d\ (i,j)}$ are the corrected estimates of the original GSRPs ($P_{s,m,d\ (i,j)}$) on the dth day of the mth month at grid cell ~i,j; and where $f_{m\ (i,j)}$ represents the interpolated correction factors at grid cell ~i,j for month m.

The latter approach—linear correction with sequential window (LCSW)—has been used in studies, such as Habib et al. [65] and Bhatti et al. [66]. Sequential time windows of varying lengths (e.g., 3, 5, 7, 10, 15, 20, 25, 30, 40, and 50 days) are tested first, and the 15-day length is found to be the most appropriate for bias correction. Therefore, the correction factors for each 15-day sequential time window throughout the study period are calculated at each gauge station as follows:

$$f_{l,k} = P_{g,l,k} / P_{s,l,k} \tag{11}$$

where $f_{l,k}$ is the correction factor for 15-day sequential time window l at station k; and where $P_{g,l,k}$ and $P_{s,l,k}$, respectively, are the accumulated rainfall amounts for the gauge and satellite in time window l at station k. After calculating the correction factors at the gauge locations, their spatial distribution over the grid cells at each sequential time window l is obtained by applying IDW interpolation. Finally, the corrected GSRPs are calculated in a temporally and spatially coherent manner, as follows:

$$P_{scor,l,d\ (i,j)} = f_{l\ (i,j)} * P_{s,l,d\ (i,j)} \tag{12}$$

where $P_{scor,l,d\ (i,j)}$ represents the corrected estimates of the original GSRPs ($P_{s,l,d\ (i,j)}$) on the dth day of the lth time window at grid cell ~i,j; and where $f_{l\ (i,j)}$ represents the interpolated correction factors at grid cell ~i,j for time window l.

4.2.2. Modified Linear Correction (MLC) Method

This method is based on the linear correction method; the correction factors at each gauge station are computed at a daily time step (instead of based on the length of the time window) using arithmetic differences rather than the ratio of the gauges to the GSRPs. Vila et al. [67] also used this method to correct TRMM 3B42RT satellite estimates for continental South America. That study featured cell-by-cell bias correction with the interpolated gauge observations, but this study's interpolation is conducted with the correction factors (arithmetic differences) calculated at the gauge stations; accordingly, the correction equations are modified as follows:

$$D_{d,k} = P_{g,d,k} - P_{s,d,k} \tag{13}$$

where $D_{d,k}$ is the correction factor for day d at station k; and where $P_{g,d,k}$ and $P_{s,d,k}$ are, respectively, the gauge and GSRP estimates for day d at station k. After calculating the values for each day and each

station, the correction factors are spatially distributed using the IDW interpolation method, and the bias-corrected GSRPs are finally calculated as follows:

$$P_{scor,d\ (i,j)} = D_{d\ (i,j)} + P_{s,d\ (i,j)} \tag{14}$$

where $P_{scor,d\ (i,j)}$ represents the corrected estimates of the original GSRPs $(P_{s,d\ (i,j)})$ on the dth day at grid cell ~i,j; and where $D_{d\ (i,j)}$ represents the interpolated correction factors at grid cell ~i,j for day d.

4.2.3. Quantile Mapping (QM) Method

The QM is a non-parametric bias-correction method that corrects errors in the shape of the distribution and that is therefore also capable of correcting errors in variability [68]. QM originates from empirical transformation [68] and has been successfully implemented in various hydrological applications [68–72]. The GSRPs at the gauge stations are adjusted using this method based on a monthly-grouped, daily-constructed empirical cumulative distribution function (*ECDF*). Specifically, the *ECDF* of each GSRP is adjusted to match with the *ECDF* of the gauge rainfall [73]. This adjustment at the gauge stations can be expressed in terms of *ECDF* and its inverse (*ECDF*$^{-1}$) as follows:

$$P_{scor,m,d,k} = ECDF^{-1}{}_{g,\ m,k}[ECDF_{s,m,k}(P_{s,m,d,k})] \tag{15}$$

where $ECDF_{s,m,k}$ is the *ECDF* of the GSRP estimates $(P_{s,m,d,k})$ at station k on the dth day of the mth month; and where $ECDF^{-1}{}_{g,\ m,k}$ is the inverse *ECDF*, corresponding to $P_{scor,m,d,k}$, which is the corrected rainfall for $P_{s,m,d,k}$ on the dth day of the mth month at station k. Rather than interpolating the QM-corrected GSRP estimates from the gauge stations to the grid cells, these estimates are instead employed with the MLC method to obtain a spatially distributed rainfall for each grid cell. In the first step, at each gauge station, the difference between gauge- and QM-corrected GSRPs is calculated for each time step (daily) and then distributed them spatially to each grid cell by applying the IDW interpolation. In the end, the gridded differences are added to the original GSRPs to produce the final version of the bias-corrected rainfall for each grid cell.

4.3. Merging of GSRPs

Hasan et al. [74] showed that merging different satellite rainfall products can reduce errors and increase performance, compared to the use of a single product. Given this finding, in this study, a number of merging techniques are applied to the GSRPs to examine whether merging various products can produce a new reference dataset with increased accuracy, which could, in turn, lead to long-term hydrological applications. To capture the spatial and temporal variations in the performance of the GSRPs, this merging is performed dynamically in this study. The final merged product for each grid cell is calculated as follows:

$$P_{mrgd,d(i,j)} = \sum_{s=1}^{n} w_{s,m,\ (i,j)} * P_{s,m,d\ (i,j)} \tag{16}$$

where $P_{mrgd,d(i,j)}$ is the merged rainfall estimate on the dth day at grid cell ~i,j, n is the number of GSRPs; $w_{s,m,\ (i,j)}$ is the weight calculated for the GSRP s in month m at grid cell ~i,j; and $P_{s,m,d\ (i,j)}$ is the rainfall estimate of the GSRP s on the dth day of the mth month at grid cell ~i,j.

Three merging techniques—simple average (SA), error variance (EV), and inverse error variance weighting (IEVW)—are used in this study to calculate the weights of the individual GSRPs at each gauge location. In the first step, the GSMaP-G and MSWEP products (which have 0.1° spatial resolution) are aggregated into the 0.25° resolution (which is what the other two products, CHIRPS and TMPA-G, use) to ensure a common resolution for the merged product. The 0.25° resolution is selected because it is coarser resolution over which two of the GSRPs (CHIRPS and TMPA-G) are distributed, meaning that an aggregation of the GSMaP-G and MSWEP products from 0.1° resolution to 0.25°—does not produce uncertainty. In the second step, as with the bias-correction techniques,

the merging weights of the individual GSRP are calculated at the gauge stations and then interpolated (using the IDW method) to each grid cell of the basin to obtain a spatially distributed merged product. A brief description of the three merging techniques is detailed below.

4.3.1. Simple Average (SA) Merging

Satellite rainfall products often show varying performance due to overestimation or underestimation of rainfall. However, researchers have found that using simple averaging for various forecasts in a microeconomic time series can outperform more complicated weighting schemes involving the individual datasets [75–77]. Therefore, simple averaging of the GSRPs can produce an improved dataset. The merging weights of the individual GSRPs are calculated in this method as follows:

$$w_{s,m, (i,j)} = 1/n \tag{17}$$

where $w_{s,m, (i,j)}$ is the weight of satellite product s in month m at grid cell $\sim i,j$; and where n is the number of GSRPs. This method is the simplest, as it is static, with the weights being equal for each GSRP and for each month depending only on the number of products.

4.3.2. Error Variance (EV) Merging

Following the techniques that Hasan et al. [74] and Woldemeskel et al. [78] implemented in their studies, the EV method used in this study is extended to be used for multiple products in a dynamic form. More specifically, to capture the spatiotemporal variation of the satellite products, the daily rainfall values for both the gauges and the GSRPs are grouped monthly. Then, the variance of the errors between the gauges and the satellite products are estimated for each month at each gauge station and then spatially distributed to each grid cell using the IDW interpolation method. The weight for each product is finally calculated as follows:

$$w_{s,m, (i,j)} = \frac{1}{n-1} * \frac{\sum_{s=1}^{n} var_{s,m,(i,j)} - var_{s,m,(i,j)}}{\sum_{s=1}^{n} var_{s,m,(i,j)}} \tag{18}$$

where n is the number of GSRPs; $var_{s,m,(i,j)}$ is the error variance of the GSRP s for which the weight $w_{s,m, (i,j)}$ is calculated in the mth month at grid cell $\sim i,j$; and $\sum_{s=1}^{n} var_{s,m,(i,j)}$ is the summation of the error variances for all GSRPs in month m at grid cell $\sim i,j$.

4.3.3. Inverse Error Variance Weighting (IEVW) Merging

Shen et al. [79] implemented this method to evaluate the performance of various satellite datasets on the Tibetan Plateau. The formula is slightly modified in our study, with the sum of the weights of each product set to unity so that the merged product remains unbiased. As with the EV method, this is also dynamic; the monthly weights are calculated as follows:

$$w_{s,m, (i,j)} = \frac{1/var^2_{s,m,(i,j)}}{\sum_{s=1}^{n} 1/var^2_{s,m,(i,j)}} \tag{19}$$

where the symbols in this equation are the same as those in Equation (18).

4.4. Combination of Merging and Bias Correction

In this study, a combination of merging and bias correction is also applied to the GSRPs to examine whether a more accurate rainfall dataset can be generated for the Meghna basin to be used in long-term hydrological applications. Among the merged products produced from the three merging techniques, the product that provides the best results is then further corrected using the best-performing bias-correction method of those discussed above.

4.5. Performance Evaluation of the Bias-Corrected and Merged Products

The overall performance of the improved products (both bias-corrected and merged) is evaluated using Taylor's diagram [80], which summarizes the statistical differences between the time series of ground rainfall and the satellite estimate. The diagram concludes how fair the satellite-based rainfall estimates relate to the gauge estimates in terms of three statistical indicators: normalized root mean square difference (NRMSD), series normalized standard deviation (NSD), and correlation coefficient (CC). This diagram is useful for summarizing the statistical-error performances in a single 2D plot.

4.6. Streamflow Simulations

In this study, a distributed hydrological model called the rainfall-runoff-inundation (RRI) model is used to perform streamflow simulations. RRI is a 2D model capable of simulating rainfall-runoff and flood inundation simultaneously [81–83]. The model deals with slopes and river channels separately. At a grid cell where a river channel is located, the model assumes that both the slope and river are positioned within the same grid cell. The channel is discretized as a single line along the centre line of the overlying slope grid cell. The flow for the slope grid cells is calculated using a 2D diffusive-wave model, and the channel flow is calculated using a 1D diffusive-wave model. For better representations of RRI processes, the model also simulates lateral subsurface flow, vertical infiltration flow, and surface flow. The lateral subsurface flow, which is typically most important in mountainous regions, is treated in terms of the discharge-hydraulic gradient relationship, which takes into account both the saturated subsurface flow and the surface flow. On the other hand, the vertical infiltration flow is estimated using the Green-Ampt model. The flow interaction between the river channel and the slope is estimated based on various overflowing formulae, which depend on water-level and levee-height conditions.

To investigate its potential for use as a reference rainfall data in streamflow simulation for the Meghna basin, the improved rainfall dataset (created by this study) is used to calibrate the RRI model parameters for the first half of the study period (from 2009 to 2012). The observed streamflows at Bhairab Bazar station are used to fit the model simulations for the calibration period. The calibration is first performed with the default parameters of the model, and the parameters are then finalized according to the best-fit hydrographs and several performance indicators. The parameters for the RRI model's calibration are mainly grouped into two kinds: (1) river-channel parameters and (2) surface- and subsurface-flow parameters. The former type incorporate aspects of river geometry such as river width, river depth, bank height, and channel roughness. The latter type consist of the properties of the land surface layer (roughness), subsurface layer (soil depth, porosity), vertical infiltration (vertical hydraulic conductivity, etc.), and lateral subsurface flow (lateral hydraulic conductivity, porosity, etc.).

Using the calibrated model parameters, the validation of the RRI model is also performed by generating streamflows with the improved dataset for the latter half of the study period (from 2013 to 2016). The results are then compared with the observed streamflows at Bhairab Bazar station. In addition, an additional validation of the RRI model is also conducted by comparing the observed streamflows with those of the model for the Amalshid stream gauge station (the Meghna River's prime entrance point into Bangladesh from India) for the entire study period (2009–2016). This allows for a further check of the model's performance and of the potential for the rainfall dataset to be used when simulating flood flows inbound from India.

5. Results and Discussion

To carry out the performance evaluation of the GSRPs and to investigate their potential for use as a reference rainfall dataset in the Meghna basin, this study compares each of the GSRPs with the ground rainfall measurements at the gauge locations on a point-to pixel basis. However, rain gauges are available only at 20 locations within the Bangladesh portion of the basin. Therefore, the performance of the GSRPs is evaluated at only these 20 gauge stations. The evaluation is conducted for the wet season at the daily and monthly temporal scales throughout the study period (2009–2016). After the

performance check, several bias-correction and merging techniques are applied to the GSRPs to create a set of improved rainfall datasets. In addition, a combined use of merging and bias correction is also explored. Finally, of the bias-corrected and/or merged products, the product that provides the best results, is used to run the RRI hydrological model, which simulates streamflows at two critical locations in the basin. The results of the analyses and the related discussion are as follows.

5.1. Performance Evaluation of GSRPs on the Daily Scale

The rainfall-detection ability of the GSRPs (compared to the gauge records) is estimated based on the categorical statistics described in Section 4.1. The estimation is collectively conducted for all of the 20 rain-gauge stations, and the results are summarized in Table 3. Relative to the gauge records, GSMaP-G and MSWEP outperformed CHIRPS and TMPA-G by detecting more rainy days (Table 3, differences measured using POD). However, the former two products detected more non-rainy days as well (Table 3, differences are measured using FAR). As shown in Table 3, SR and TS indicate no significant disparities among the GSRPs.

Table 3. Categorical statistics calculated for daily GSRP rainfall estimates relative to daily ground rainfall in the wet season throughout the study period (2009–2016).

Categorical Statistic	Scores				Perfect Score
	CHIRPS	GSMaP-G	TMPA-G	MSWEP	
Probability of Detection (POD)	0.69	0.98	0.79	0.98	1
Strike Ratio (SR)	0.71	0.62	0.75	0.65	1
False alarm ratio (FAR)	0.35	0.47	0.33	0.45	0
Threat score (TS)	0.50	0.52	0.57	0.54	1

Figure 4a–t compares the cumulative rainfall of the ground gauges, CHIRPS, GSMaP-G, TMPA-G, and MSWEP daily estimates at each gauge station calculated for the wet season throughout the study period (2009–2016). The plotting order is based on the varied (extreme- to low-) intensity of the mean annual gauge rainfall (Table 1). The results show varying performance, with the GSRPs either over- or under-estimating cumulative rainfall relative to the gauge rainfall at most of the stations—although nearly accurate estimates are also observed at some of the stations. CHIRPS tends to overestimate cumulative rainfall relative to gauge rainfall at most (16) of the stations (Figure 4c,e–h,j–t), regardless of gauge rainfall intensity, whereas GSMAP-G underestimates at nine stations (Figure 4a–f,i,j,p) and overestimates at six others (Figure 4k–n,q,t). TMPA-G and MSWEP, on the other hand, both underestimate (Figure 4a–f,i for TMPA-G and Figure 4b,d,f,g,i for MSWEP) and overestimate (Figure 4g–h,j–o,q–t for TMPA-G and Figure 4a,e,h,k,l,n,o,q–t for MSWEP) the cumulative rainfall at the stations in times of both high- and low-intensity of gauge rainfall.
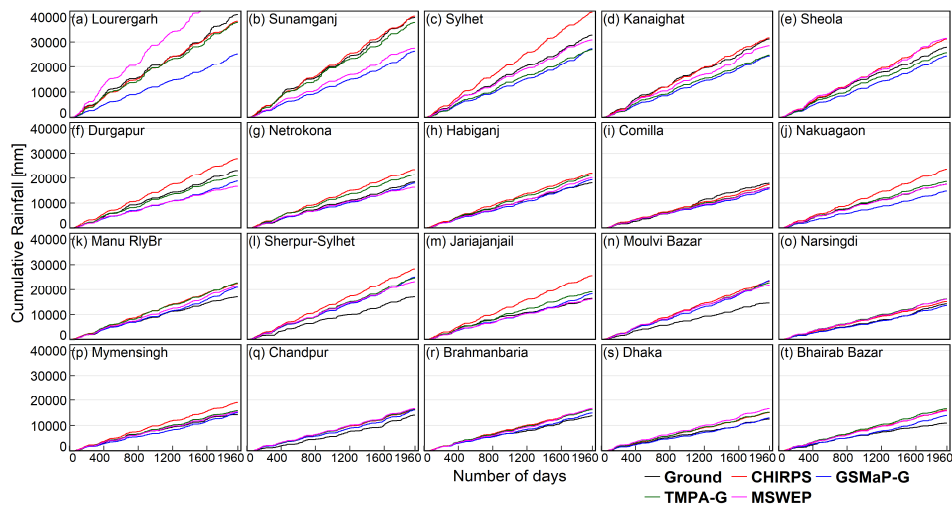
Figure 4. Cumulative rainfall of daily estimates calculated for the ground gauges and GSRPs throughout the wet season (March–October) of the study period (2009–2016), at 20 rain-gauge stations (**a**–**t**) located within the Bangladesh portion of the Meghna basin.

Using the indices based on Equations (1)–(4) in Section 4.1, Figure 5a–t compares daily CHIRPS, GSMaP-G, TMPA-G, and MSWEP estimates for the wet seasons during the entire study period against the daily ground rainfall measurements at 20 rain-gauge stations. The results once again show varying performance for daily estimates of each product. According to the calculated statistics, each product performs differently, resulting in both positive and negative relative biases (RB) in extreme- as well as low-rainfall areas. The accumulated errors (i.e., NMSE and RMSE) for each product result in high magnitudes at all stations and indicate no significant disparities among the products. The errors of agreement (the calculated CCs) show very low coherence for CHIRPS and slightly better (but still low) coherence for the other three products at all gauge stations.
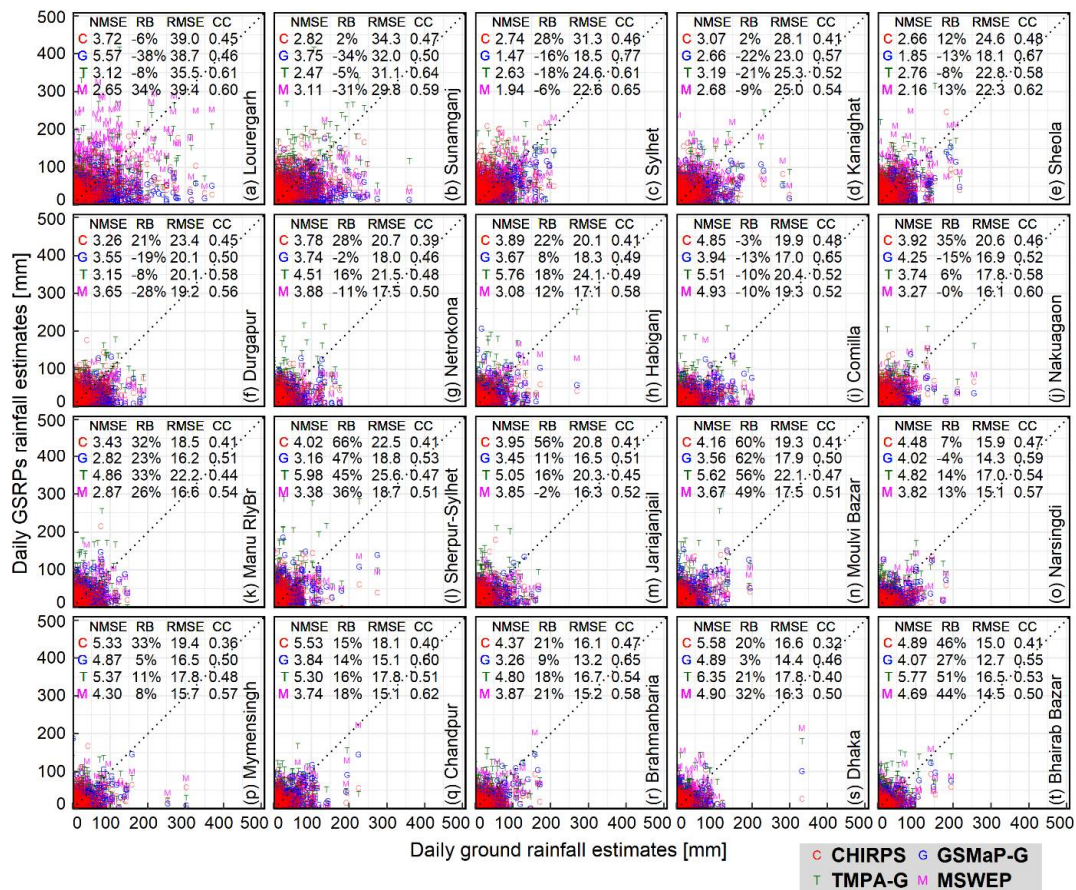
Figure 5. Scatterplots of daily GSRP estimates against daily ground rainfall for the wet seasons during the entire study period (2009–2016) at 20 rain-gauge stations (**a**–**t**). Comparison indices are included inside the plot for each station.

5.2. Performance Evaluation of GSRPs on the Monthly Scale

Figure 6a–t presents a comparison of mean monthly accumulated estimates for CHIRPS, GSMaP-G, TMPA-G, and MSWEP relative to the ground rainfall records at each gauge station. Unlike with the daily rainfall accumulations, the monthly accumulations of all products have lower NMSE and show greater coherence (measured using CC) relative to the ground rainfall. This indicates that the GSRPs accurately estimate the mean monthly accumulated rainfall. On the other hand, the monthly accumulations of all the products follow the daily trend and show insignificant disparities in calculating RMSE. The relative bias (RB) results for the monthly accumulations, are the same as for the daily accumulations, as RB is calculated for the entire study period (2009–2016) in both cases.
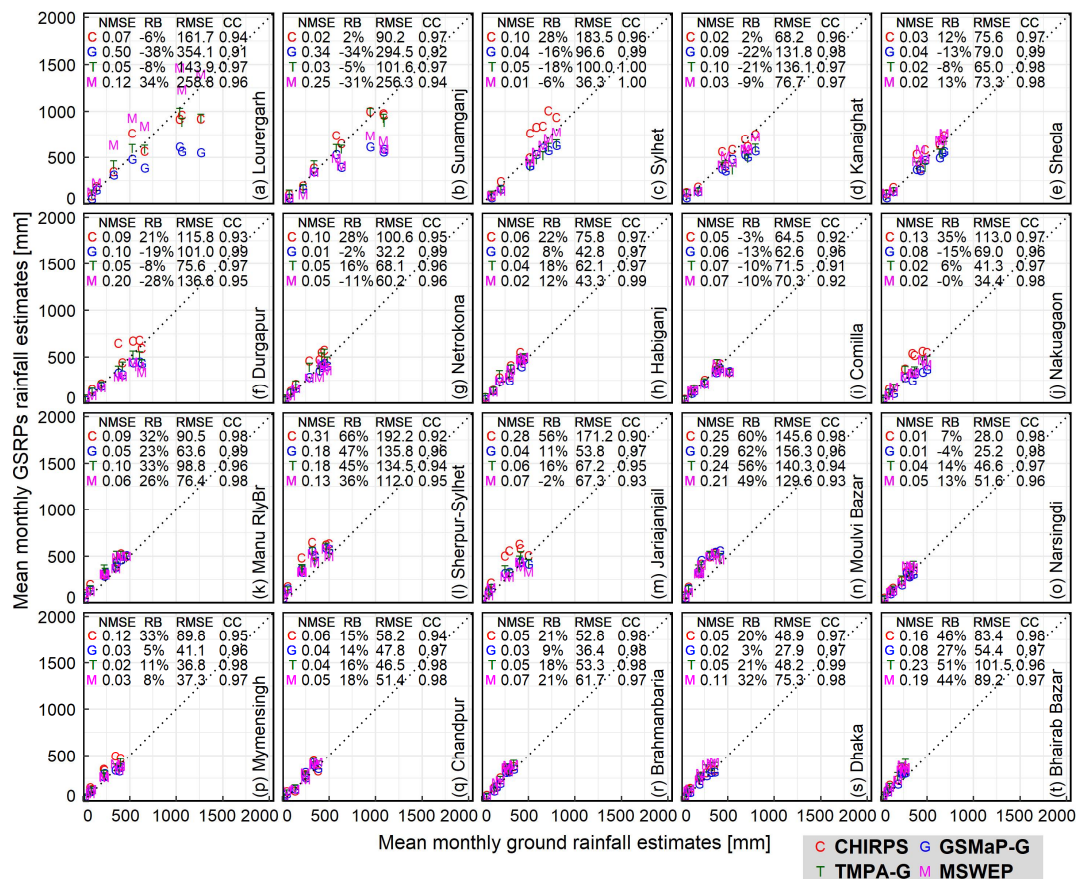
Figure 6. Scatterplots of mean monthly accumulated GSRP estimates against the ground rainfall for the wet seasons during the entire study period (2009–2016) at 20 rain-gauge stations (**a**–**t**). Statistical indices are included inside the plot for each station.

Figure 7a–t compares mean monthly ground rainfall to the GSRP estimates at 20 rain-gauge stations for the months of rainy season (March–October) during the study period (2009–2016). The results, which show that the mean monthly rainfall of the gauge stations, that experienced medium to low rainfall intensity (Figure 7g–t), fit with the mean monthly accumulated rainfall of the GSRPs reasonably well for almost all of the rainy months. On the other hand, at nearly all the gauge stations that experienced extreme rainfall (Figure 7a–f), CHIRPS overestimates the monthly rainfall, GSMaP-G underestimates it, and TMPA-G and MSWEP both over- and underestimates it. The results also show that the stations located in the farthest northeastern part of Bangladesh experienced extreme rainfall in the Bangladesh portion of the basin (Figures 2 and 7a–f).
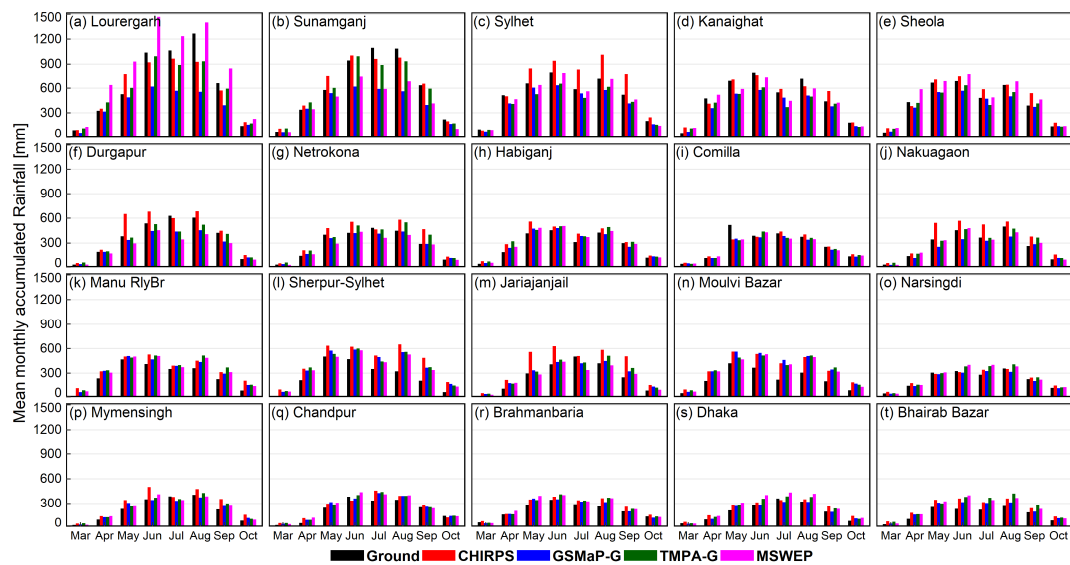
Figure 7. Mean monthly accumulated rainfall of the ground gauges and CHIRPS, GSMaP-G, TMPA-G, and MSWEP for the months of the rainy season (March–October) during the study period (2009–2016) at 20 gauge stations (**a**–**t**).

From the discussion in this section, it is observed that all of the GSRPs show a significant amount of bias (either positive or negative), as compared to the ground rainfall measurements, on both the daily and the monthly temporal scales and at each gauge station (regardless of station's topographical location or rainfall intensity). In addition, all the GSRPs largely detected the non-rainfall events. It is, thus, rational to correct the bias of the GSRPs so that they can be used as reference rainfall datasets for long-term hydrological applications in the Meghna basin. For this purpose, local rain-gauge data from 20 stations are used.

5.3. Evaluation of Bias-Corrected GSRPs

Each bias-correction technique described in Section 4.2 is applied to the original GSRPs to produce a set of bias-corrected rainfall datasets for the Meghna basin. Fifteen out of the 20 rain gauge stations are used to implement the bias correction techniques, and the remaining five stations are taken out for the validation of the correction techniques. Four experiments are conducted to select the five validation stations randomly, and these are conducted to make sure that every station is taken out once in all the experiments. However, the performance of the correction methods does not vary much in any of the combination of the validation stations. As a result, to keep the manuscript concise, one experiment with five randomly-selected validation stations (that include Sunamganj, Sheola, Nakuagaon, Brahmanbaria, and Bhairab Bazar (Table 1)) is presented in this study. Figure 8a–e shows Taylor diagrams [80] with a comparison of the original and bias-corrected daily estimates for the GSRPs with those of the ground gauges at the five validation stations for the rainy seasons of 2009–2016. The purpose of this diagram is to show the temporal variability of the satellite estimates (both the original and corrected GSRPs) relative to the ground-based observed rainfall, in terms of NRMSD, CC, and NSD. According to Taylor [80], the grey straight lines in Figure 8a–e display the CC of the satellite estimates; the blue dotted arcs are the NRMSD; the green dotted arcs display the NSD of the satellite estimates; the black dashed arc line denotes the NSD of the observed fields; satellite estimate patterns which agree well with the observed field's pattern lie close to a point marked obs on the *x*-axis, indicating a relatively high correlation and a low NRMSD; and the NSD of satellite estimates, matching the observed-based NSD, have patterns with the right amplitude. The results indicate that the linear correction method based on the mean monthly time window (LCMW) mostly fails to correct the satellite estimates (blue symbols), relative to the original GSRPs (red symbols); this method, thus,

shows no significant improvements in terms of the performance indicators (CC, NRMSD, and NSD). Likewise, the linear correction method based on the sequential time window (LCSW) cannot correct the bias of the GSRPs (green symbols), compared to the original GSRPs (red symbols), although LCSW performed slightly better than LCMW in terms of removing systematic biases from the original GSRPs. The quantile mapping (QM) correction method adopted in this study outperforms the linear correction methods and lead to improved indices (orange symbols) compared to the original GSRPs (red symbols). Higher correlations (in CC), lower NRMSD, and lower variability (in NSD) are observed at all five validation stations for all of the GSRPs after correction with the QM method. However, the modified linear correction (MLC) method shows significant improvements in removing systematic biases from the GSRPs (black symbols) and outperforms both the linear and QM correction methods. The NRMSD and NSD errors for the validation set decrease with the MLC method, and the CCs indicate greater coherence than in the original GSRPs. Although all of the GSRPs are corrected comparatively well in the MLC method, the TMPA-G provides better results than the other three products (GSMaP-G, CHIRPS, and MSWEP).
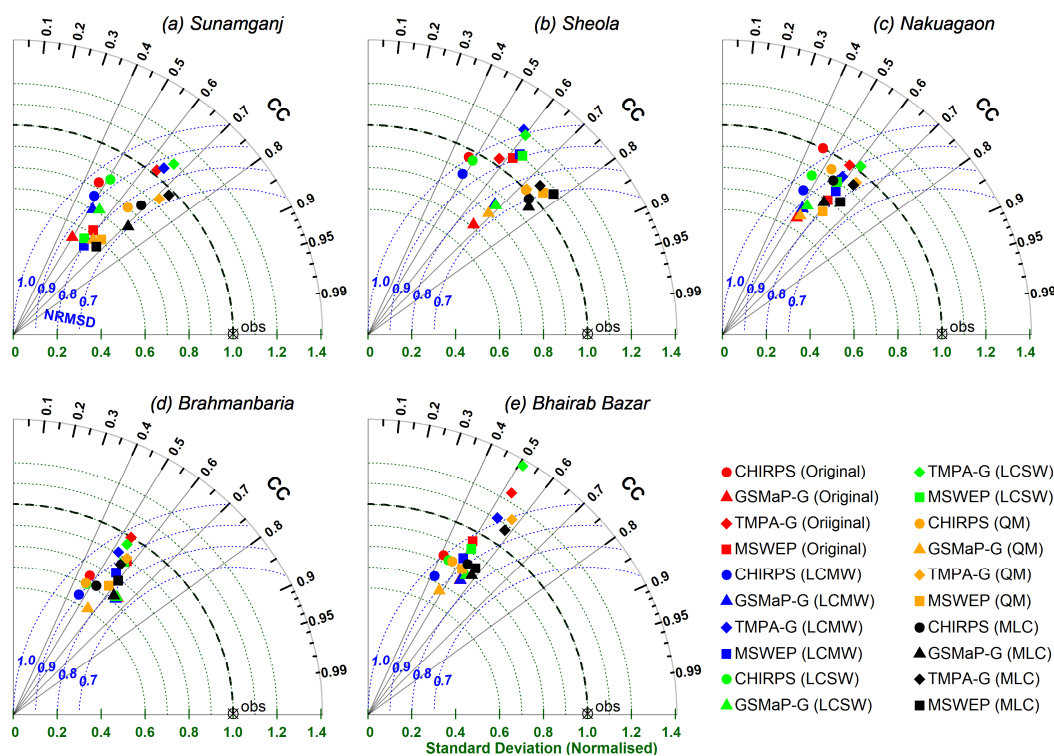

Figure 8. Taylor diagram illustrating statistical comparison between original, bias-corrected GSRP estimates and gauge rainfall (obs mark), as calculated for the wet seasons of 2009–2016 at five validation stations (**a**–**e**). The CCs are related to the azimuthal angle (grey lines), which denote a similarity in pattern between the satellite and gauge fields. NSDs (green contours) indicate the amount of variance between the satellites and the gauge time series, and is proportional to the radial distance from the origin. The NRMSD (blue contours) between the satellite products and the rain-gauge fields is proportional to the distance from the point on the *x*-axis identified as obs. For details, refer to Taylor [80].

5.4. Evaluation of Merged Products

Researchers have shown that merging satellite rainfall products can reduce errors and increase performance relative to any individual product. Hence, three merging techniques—SA, EV, and IEVW, laid out in Section 4.3—are applied to the original GSRPs to see if merging alone can produce an improved dataset relative to both the original and the bias-corrected GSRPs. The daily estimates of the

three merged products are compared with those of the gauges at the 20 gauge stations for the rainy season throughout the study period. Figure 9a–t shows Taylor diagrams with statistical comparisons between satellite estimates (both original GSRPs and merged products) and observed rainfall at the gauge stations. As shown in the figures, the results indicate that merging the GSRPs can significantly reduce the biases of the individual product relative to the ground rainfall. Compared to the original GSRPs (bubbles), the products of all three merging methods (triangles) result in improved statistical indices at each gauge station. Even the SA method, which does not use any ground rainfall records, provides better results (magenta triangle) than any individual GSRP provides. This may be due to the fact that combining the GSRPs leverages the mutual strengths of each product to create a more representative product. Although all three merging methods perform well in reducing errors from the original GSRPs relative to the ground rainfall, the IEVW (black triangle) performs better than the SA and EV methods.
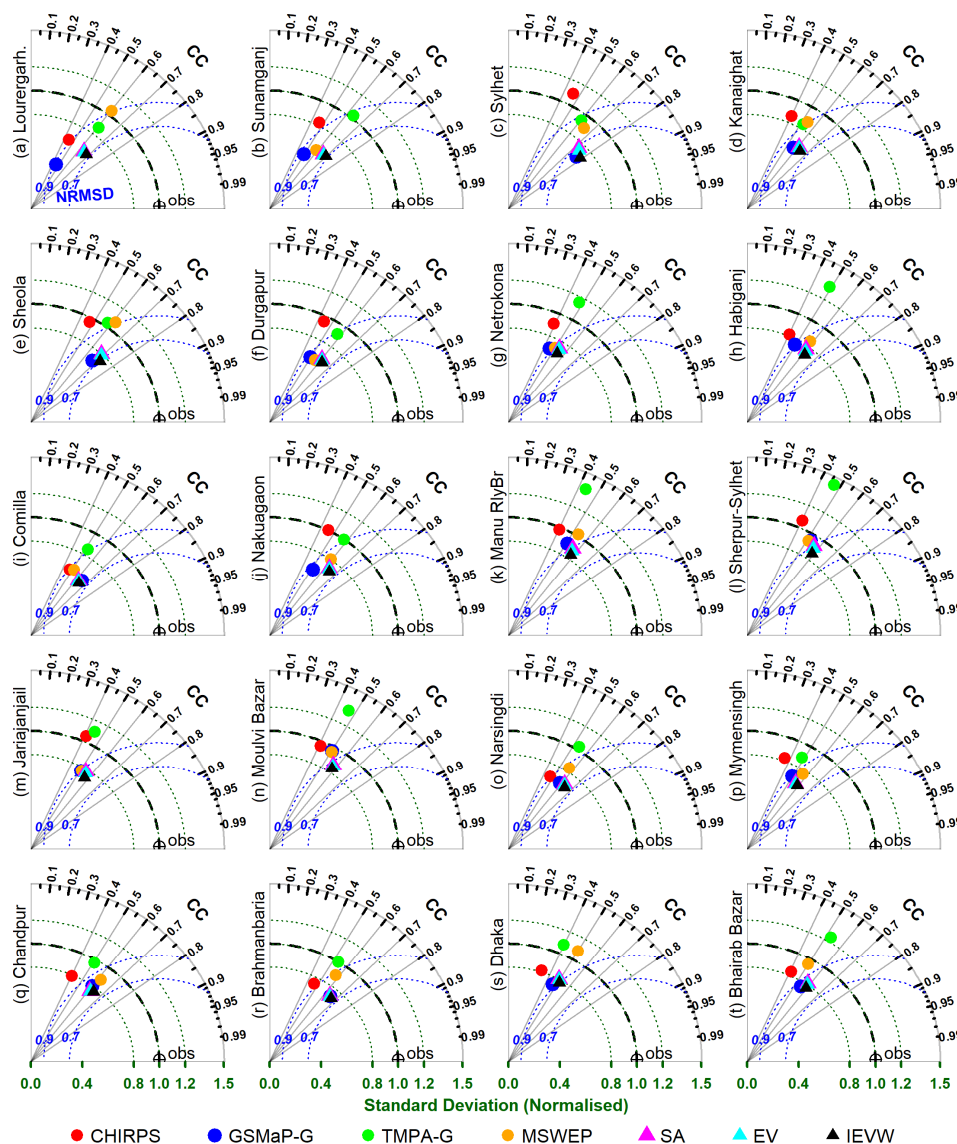

Figure 9. Taylor diagram illustrating a statistical comparison between satellite products (original and merged) and ground rainfall (obs mark) for the wet seasons of 2009–2016 at 20 rain-gauge stations (**a**–**t**). Instructions for reading a Taylor diagram are given in Figure 8.

5.5. Combined Use of Merging and Bias Correction

As discussed in Section 5.4, the merging of the GSRPs improves the data and performs better (with increased indices) than any individual product does. All three of the merging techniques produce representative datasets, with IEVW outperforming SA and EV. On the other hand, as discussed in Section 5.3, the original GSRPs are best corrected using the MLC bias-correction method. This method improves the accuracy of the products and reduces errors significantly. However, among the five validation stations, Sunamganj and Sheola, which both experienced extreme rainfall, show better results (higher CC and lower NRMSD) for the MLC-corrected GSRPs than for the IEVW-based merged product (Figure 8a,b and Figure 9b,e). On the other hand, the IEVW-based merged product produces improved indices (higher CC and lower NRMSD) at the remaining three stations (Figure 8c,d,e and Figure 9j,r,t)—those that experienced medium to low intensity of rainfall. Therefore, the IEVW merging technique followed by the MLC bias-correction method is explored to examine whether the combined use of merging and bias correction can produce an improved dataset with increased performance and applicability. Figure 10a–e shows Taylor diagrams with statistical comparisons between time series for the satellite products (original GSRPs; MLC corrected GSRPs; and IEVW-based merged products (both without and with the MLC bias correction)) and ground rainfall at the five validation stations for the rainy seasons of 2009–2016. The results show improvements for the combined product that employs both merging (IEVW) and bias-correction (MLC) techniques. Compared to the errors (CC, NRMSD, and NSD) produced with the original GSRPs (red symbols), the MLC-corrected GSRPs (blue symbols), and the IEVW-merged product of the original GSRPs (magenta symbol), the combined product (black symbol) results with improved indices (higher CC, lower NRMSD, and relatively lower NSD) at each of the five validation stations, which indicates that the combined use of merging and bias correction can produce an improved dataset for various hydrological applications in the Meghna basin.
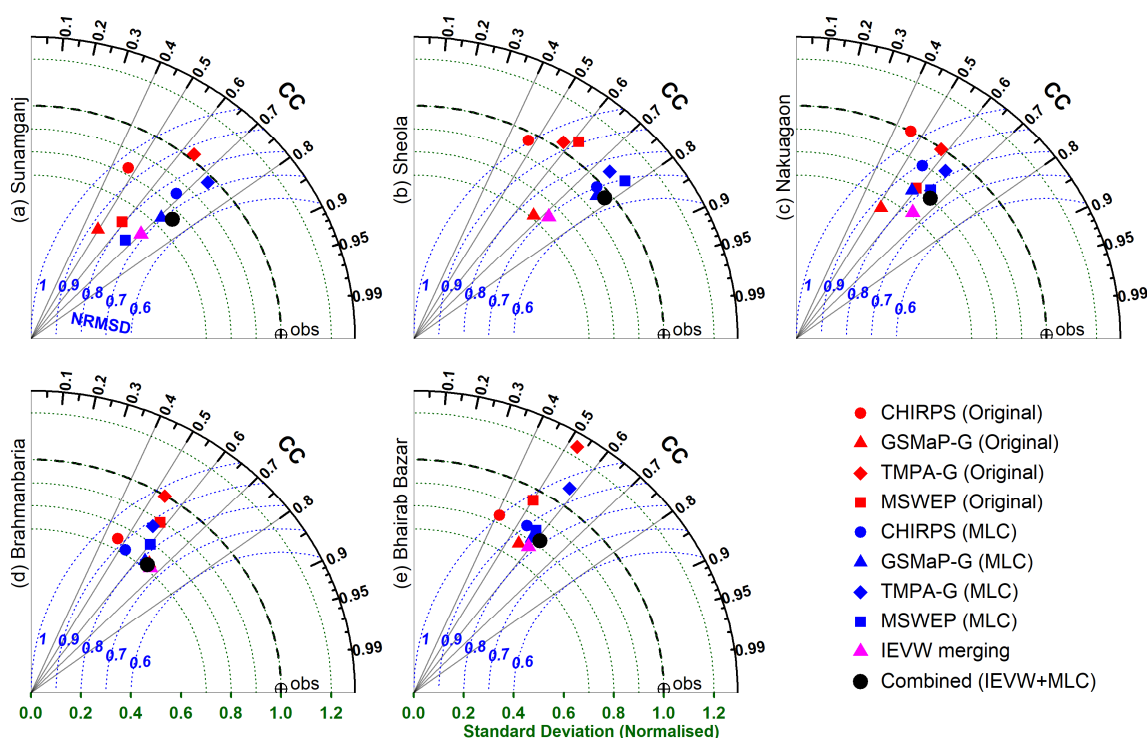

Figure 10. Taylor diagram with the statistical comparison of the original GSRPs, the MLC-corrected GSRPs, and the IEVW-based merged product of the original GSRPs (both without and with the MLC bias correction) against ground rainfall for the wet seasons of 2009–2016 at the five validation stations (**a**–**e**). Instructions for reading a Taylor diagram are given in Figure 8.

The improved dataset, which is created in this study by combining the IEVW merging technique and the MLC bias-correction method (the dataset hereafter called IMLC), is finally compared with the original GSRPs relative to the ground rainfall measurements for daily, monthly, and annual time series; this is done to evaluate the overall temporal representation and variability of the satellite rainfall estimates. Figure 11a–c shows Taylor diagrams with a statistical comparison of the original GSRPs and the IMLC product relative to the ground rainfall, collectively calculated for the five validation stations—in terms of (a) daily, (b) monthly, and (c) annual accumulated rainfall—for the entire study period of 2009–2016. As with the original GSRPs, the best agreement for the IMLC product in terms of correlation, is in monthly accumulated rainfall. All the original GSRPs capture the monthly rainfall amount reasonably well, and have CCs ranging from 0.89 to 0.97; by comparison, the monthly rainfall of the IMLC product alone shows a CC of around 0.97. On the other hand, the daily correlations for the GSRPs are found considerably lower, with no dataset showing a CC greater than 0.6, whereas the daily rainfall of the IMLC product shows a higher CC of about 0.75. The annual accumulated rainfall has lower correlations for the GSRPs, with the exception of CHIRPS and TMPA-G, leading to a CC at the same level as the IMLC product: about 0.95. All the GSRPs and the IMLC product underestimate the inter-daily, -monthly, and -annual variability—in other words, the NSD of the daily, monthly, and annual rainfall—except for the daily variability, which TMPA-G overestimates. However, in all three time scales, IMLC shows lower variability than the GSMaP-G and MSWEP products; it also produces minimal variation that is nearly the same as what is found in the CHIRPS and TMPA-G products. The ranking of NRMSD for the GSRPs varies depending on the time scale; however, compared to GSMaP-G and MSWEP, CHIRPS, and TMPA-G show relatively low NRMSD errors for the monthly and annual estimates, and relatively high errors for the daily estimates. On the other hand, the improved product, IMLC, shows considerably lower NRMSD errors than all of the GSRPs on the daily time scale, and also lower NRMSD errors than the GSMaP-G and the MSWEP products at the monthly and annual time scales, just as the TMPA-G and CHIRPS products do. Overall, the three statistics plotted in the Taylor diagram show lower NRMSDs and lower variability (in NSD), as well as higher coherence (measured with CC) for the IMLC product than any individual GSRP at all three time scales, when compared to the gauge rainfall. In particular, the daily rainfall of the IMLC product produces better indices than do the daily GSRPs, indicating IMLC's potential for use as a reference rainfall dataset in any hydrological model to simulate daily hydrological responses of the Meghna basin.
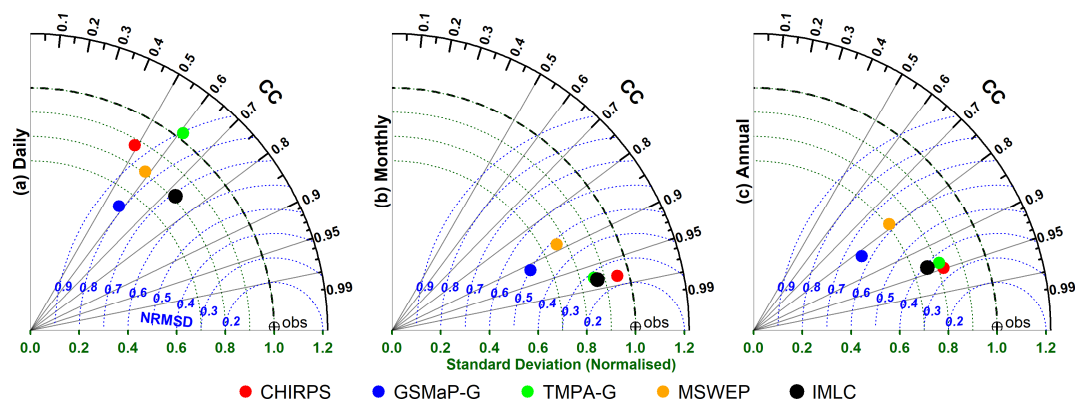

Figure 11. Taylor diagrams plotted for the (**a**) daily, (**b**) monthly, and (**c**) annual time series of the original GSRPs and the IMLC product vs. the ground rainfall collectively calculated for the five validation stations for the period of 2009–2016. Instructions for reading a Taylor diagram are given in Figure 8.

Figure 12a–e shows the gridded (0.25° resolution) annual average rainfall, as calculated from the four GSRPs and the IMLC product, for the study period of 2009–2016. The purposes of this figure are to understand the spatial distribution of the rainfall pattern by each of the GSRP products and to

check the performance of the IMLC product relative to the GSRPs. The results indicate that the IMLC product has used the respective strengths of the individual GSRPs to offset their respective weaknesses, resulting in a representative rainfall product for the basin.
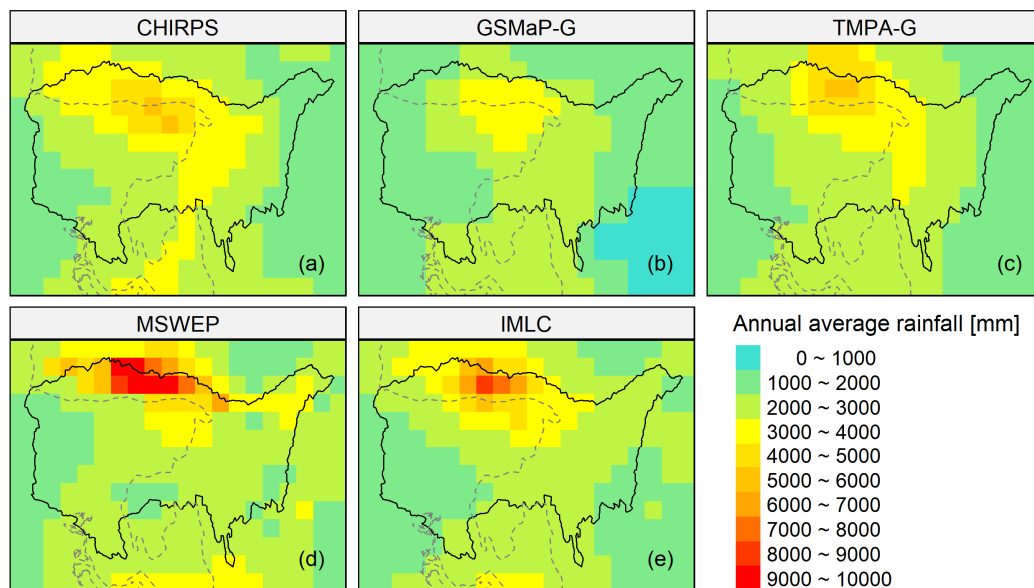

Figure 12. Annual average rainfall distribution at 0.25° grid resolution for (**a**) CHIRPS, (**b**) GSMaP-G, (**c**) TMPA-G, (**d**) MSWEP, and (**e**) IMLC product during the study period (2009–2016).

5.6. Validation of the IMLC Product Outside of Bangladesh

As discussed earlier, India does not share any kind of hydro-meteorological data with Bangladesh, officially. Therefore, we could not validate the satellite time series (either the GSRPs or the IMLC product) at either spatial or temporal scale outside the Bangladesh portion of the Meghna basin. However, the India Meteorological Department shares some customized rainfall information on its website (http://www.imd.gov.in/); for example, it shares the district-wise monthly average rainfall, and the district-, subdivision-, and state-wise weekly accumulated rainfall. The monthly average rainfall figures are available for the last five years, whereas the weekly rainfall for the past week is given online only for the current time. The district-wise monthly average rainfall figures are calculated based on the arithmetic averages of the monthly accumulated rainfall values for the stations located in that district. Among the 26 districts that lie fully or partially within the Indian part of the Meghna basin, the monthly average rainfall of nine districts (e.g., South Garo Hills, West Khasi Hills, East Khasi Hills, Jaintia Hills, Cachar, Karimganj, Hailakandi, North Tripura, and Dhalai; Figure 1a) is compared with the corresponding district-average monthly rainfall figures derived from the GSRPs and from the IMLC product for the period of 2012–2016 (five years). Figure 13a–i shows Taylor diagrams that compare the district-average monthly time series of the satellite products (both the original GSRPs and IMLC) against that of the observed rainfall for the aforementioned nine Indian districts. Of the three indices (NRMSD, NSD, and CC) shown in the Taylor diagrams, NRMSD and NSD errors are lower and CC is higher for the IMLC product than for each of the GSRPs in every district, which indicates IMLC's strength in detecting the magnitude and spatio-temporal distribution of monthly rainfall in the Indian portion of the basin.
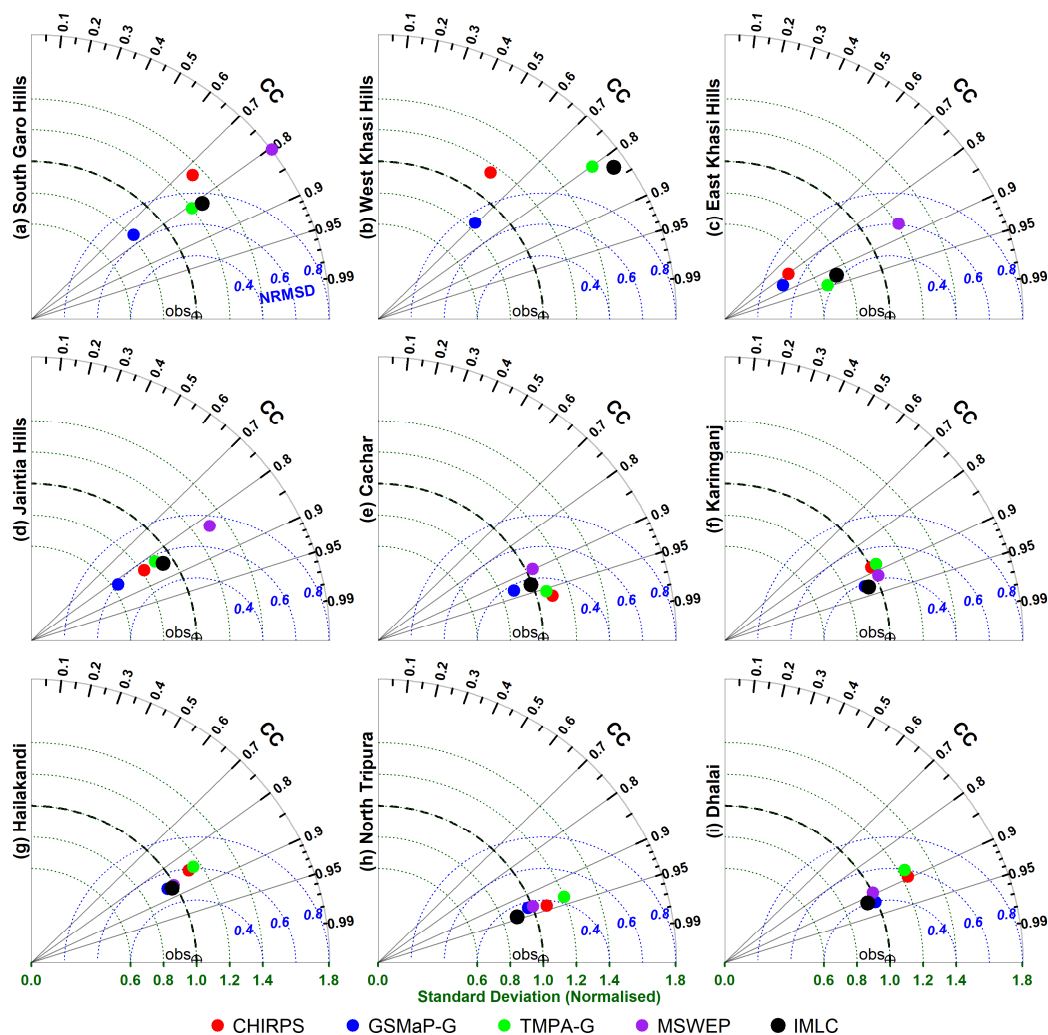
Figure 13. Taylor diagram with a comparison of the monthly accumulated district-average rainfall estimates (calculated from the original GSRPs) and IMLC product (the improved dataset created in this study) relative to the observed rainfall of nine districts (**a–i**) located inside the Indian portion of the Meghna basin for the period of 2012–2016. Instructions for reading a Taylor diagram are given in Figure 8.

The IMLC dataset, which is created in this study by merging the GSRPs using the IEVW technique and applying the MLC bias-correction method, showed better spatio-temporal representation of rainfall estimates than did the individual GSRPs at all the gauge stations, including the five validation stations located inside the Bangladesh portion of the Meghna basin. In particular, the three validation stations (Sunamganj, Sheola, and Nakuagaon) that experienced heavy rainfall in the basin, all of which are located near or on the Bangladesh-India border (Figure 2), resulted in better estimations of rainfall for the IMLC product (Figure 10a–c). The IMLC product also showed improved results for monthly average rainfall estimates relative to those of observed rainfall for the nine districts in the Indian portion of the basin (Figure 13a–i). Therefore, it can be assumed that this IMLC product (which has a grid resolution of 0.25°) can provide better estimation of rainfall in all the grid cells in the basin, both inside and outside of Bangladesh. Given this assumption, the IMLC product is hereafter treated as the improved rainfall dataset for streamflow simulations in the basin.

5.7. Streamflow Simulations with the Improved Dataset (IMLC Product)

The applicability of the improved rainfall dataset is investigated by simulating streamflows at two critical stream-gauge stations in the Meghna basin using the RRI hydrological model. To produce more reliable streamflows, the parameters of the RRI model are needed to be calibrated and validated for the Meghna basin. Thus, the model is first calibrated with the improved rainfall dataset for the period of 2009–2012 at the basin's outlet, Bhairab Bazar station (Figure 1b). The model validation is also performed at this station using the improved dataset for the period of 2013–2016. Similarly, an additional validation of the model is also carried out at the Amalshid stream-gauge station (the Meghna River's prime entrance point into Bangladesh from India) for the entire period of the study (2009–2016).

Figure 14a,b shows the daily hydrographs of the observed and simulated streamflows at Bhairab Bazar station for the period of model's calibration and validation. Figure 15 shows the daily hydrographs of the observed and simulated streamflows at Amalshid station, which are plotted for the purpose of providing additional model validation and for checking the performance of the improved rainfall dataset when simulating incoming streamflows from the Indian part of the basin. The calculated model-performance indices are presented in Table 4 for the calibration, validation, and additional-validation periods. The calculated NSE is 0.93, 0.93, and 0.75, while the CC is 0.98, 0.97, and 0.86 for the calibration, validation, and additional-validation periods, respectively. The other three statistics in Table 4: RMSE, VB, and NMSE show overall satisfactory indices in all three phases. These statistical indices (Table 4), together with the hydrographs (Figures 14 and 15), reveal that the RRI model simulations using the improved rainfall dataset reproduce the timing and volume of the streamflows, as well as the seasonal, annual, peak, and low flows very well, which indicates that the improved dataset has the potential to provide accurate streamflow estimates across the basin. This improved dataset can, thus, be used as a reference rainfall dataset for long-term hydrological applications, damage assessments, and other climatic applications in the Meghna basin.
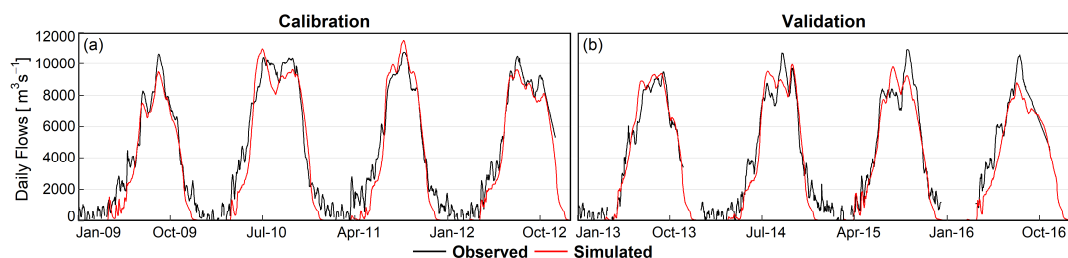

Figure 14. Daily observed streamflows (black) and simulated streamflows (red) produced by the improved rainfall dataset (the IMLC product) for the periods of (**a**) calibration (2009–2012) and (**b**) validation (2013–2016) using the RRI model at the Bhairab Bazar stream gauge. See Table 4 for the statistical metrics used to evaluate the simulated streamflows.
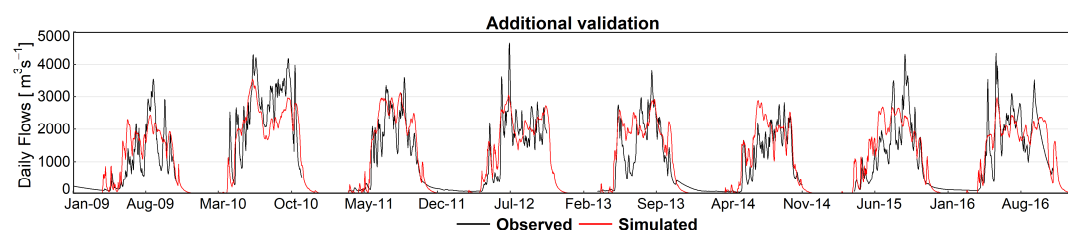

Figure 15. Daily observed streamflows (black) and simulated streamflows (red) produced by the improved rainfall dataset for additional validation of the RRI model at the Amalshid stream gauge during the entire study period (2009–2016). See Table 4 for the statistical metrics used to evaluate the simulated streamflows.

Table 4. Statistical indices used to measure the performance of the RRI model simulations in the calibration, validation, and additional-validation phases.

Rainfall Product	Errors (Units)	Bhairab Bazar Station		Amalshid Station
		Calibration (2009–2012)	Validation (2013–2016)	Additional Validation (2009–2016)
Improved rainfall dataset (IMLC product)	Nash-Sutcliffe Efficiency (NSE) (-)	0.93	0.93	0.75
	CC (-)	0.98	0.97	0.86
	RMSE (m^3 s^{-1})	994	939	537
	Volume Bias (VB) (%)	−10	−8	8
	NMSE (-)	0.04	0.04	0.22

6. Conclusions

The lack of upstream, basin-wide hydro-meteorological data for the Meghna basin makes water resource management challenging for Bangladesh. Moreover, the ground rainfall data that is available inside Bangladesh are sparse in both the temporal and spatial scales. Therefore, researchers continue to have difficulty conducting long-term hydrological and climatic applications across the basin, as a dense rainfall network that includes both the Bangladesh and Indian parts of the basin is a driving force in simulating any hydrological responses. To overcome this issue, four GSRPs (CHIRPS, GSMaP-G, TMPA-G, and MSWEP), all of which are freely available at near-present (1–3 week latency), are evaluated to create a reference rainfall dataset in the near-present time scale for various hydrological applications in the basin. The applicability of the dataset is investigated by simulating the hydrological responses of the Meghna basin so as to develop more effective water resource management.

The performance of the GSRPs is evaluated against the ground rainfall records at 20 rain-gauge stations inside Bangladesh. The evaluation is conducted at the daily and monthly temporal scales and on a point-to-pixel basis for the rainy seasons of the entire study period (2009–2016). The analyses reveal that all the products have significant weaknesses in detecting the magnitude and spatio-temporal distribution of rainfall. CHIRPS mostly overestimates the rainfall, GSMaP-G mostly underestimates it, and both TMPA-G and MSWEP show varying performance, with both over- and underestimation at the rain-gauge locations. The biases are higher at the daily scale than at the monthly scale. In the case of capturing rainfall events, the GSRPs perform considerably well, but they come up with many false alarms, too.

Several bias-correction techniques (LCMW, LCSW, MLC, and QM) are applied to improve the GSRPs' daily estimates with respect to the locally-available ground-gauge rainfall. Fifteen out of the 20 rain-gauge stations are used to implement the correction techniques, and the other five are used for validating the techniques. The correction factors are calculated at the gauge stations first; then, these station-based factors are distributed using IDW interpolation to yield grid-based factor maps for each time step. Finally, bias-corrected satellite estimates are obtained by combining the original GSRPs with the grid-based correction-factor maps. The first two correction techniques (LCMW and LCSW) show difficulties in correcting the daily GSRP estimates, which might be due to the limitations of GSRPs and to the low correlations existing between the gauges and the GSRPs. The QM method, on the other hand, outperforms both LCMW and LCSW, resulting in high performance indices. However, the MLC correction method is found better than the other three methods and considerably improves upon the daily GSRP estimates by reducing their systematic errors.

Merging of the GSRPs is investigated using three merging techniques (SA, EV, and IEVW) to check whether merging alone can produce a representative rainfall dataset with improved performance than both the original and the bias-corrected GSRPs. Merging improves the data and provides better results than the individual GSRPs. At the daily temporal scale, for which some GSRPs show overestimation of rainfall while others show underestimation, and it is appeared difficult to correct the GSRPs, merging

these products brings significant improvements. However, although the merged products show improved statistical indicators at three of the five validation stations, the corrected GSRPs (with the best-performing bias-correction method, MLC) has better results at the remaining two stations (those that experienced extreme rainfall). Therefore, a combination of merging and bias-correction technique is explored, and the use of the IEVW merging technique followed by the MLC bias-correction method produces the best results and, thus, creates an improved rainfall dataset (at 0.25° spatial and daily temporal resolution).

Using the improved rainfall dataset, the distributed RRI hydrological model is then run to generate streamflows for the basin. The generated daily streamflows are compared to the daily streamflows, as measured by two critical stream gauges (Bhairab Bazar at the basin's outlet and Amalshid at the Meghna River's prime entrance into Bangladesh from India). The simulated streamflows using the improved rainfall dataset match the observed streamflows well in both pattern and magnitude. The data reproduces the timing and volume of streamflows, as well as the seasonal, annual, peak, and low flows, reasonably well for the whole basin at the outlet (Bhairab Bazar) and for the Indian part of the basin at Amalshid stream station. This finding indicates that this improved rainfall dataset has the potential of generating accurate streamflows for the entire Meghna basin.

Since Bangladesh does not receive any reliable upstream river flow and rainfall information from India in the Meghna basin, the accurate daily streamflow generation performed with the improved rainfall dataset (created in this study out of the GSRPs) allows us to overcome the issues of poor data availability and data sharing in the basin which, in turn, helps us to quantify flood flows into Bangladesh. This improved dataset can also serve as a reference dataset for a wide range of applications in the basin (e.g., flood modelling and forecasting, irrigation planning, damage, and risk assessments, construction of hydraulic structures, and climate-change adaptation planning). In our future studies, the dataset will be used as a reference dataset for the performance evaluation of globally available NRT satellite-based rainfall products in hydrological forecasting for real-time water resource management in the basin.

Author Contributions: All authors contributed for conceiving and formulating the research; M.R., T.K., and K.T. supervised the research and provided necessary suggestions. N.M. individually created the particular methodology for merging and quantile mapping bias correction and provided the related computational scripts, literature review, descriptions, and suggestions on their applications. I.M.K. performed all the calculation and produced the results; I.M.K. and M.R. analyzed the results. This manuscript was written by I.M.K and M.R.

Conflicts of Interest: The authors declare no conflicts of interest.

References

1.　Food and Agriculture Organization of the United Nations (FAO). *Irrigation in Southern and Eastern Asia in Figures, AQUASTAT Survey-2011, FAO Water Report #37*; FAO Land and Water Division: Rome, Italy, 2012.

2.　Chowdhury, M.R. An Assessment of Flood Forecasting in Bangladesh: The Experience of the 1998 Flood. *Nat. Hazards* **2000**, *22*, 139–163. [CrossRef]

3.　Mirza, M.M.Q. Three Recent Extreme Floods in Bangladesh: A Hydro-Meteorological Analysis. *Nat. Hazards* **2003**, *28*, 35–64. [CrossRef]

4.　Shah, R.B. Ganges-Brahmaputra: The outlook for the twenty-first century. In *Sustainable Development of the Ganges-Brahmaputra-Meghna Basins*; Biswas, A.K., Uitto, J.I., Eds.; Oxford University Press: Oxford, UK, 2001; pp. 17–45.

5.　Mirza, M.M.Q.; Warrick, R.A.; Ericksen, N.J. The Implications of Climate Change on Floods of the Ganges, Brahmaputra and Meghna Rivers in Bangladesh. *Clim. Chang.* **2003**, *57*, 287–318. [CrossRef]

6.   Chowdhury, M.R.; Ward, N. Hydro-meteorological variability in the greater Ganges–Brahmaputra–Meghna basins. *Int. J. Climatol.* **2004**, *24*, 1495–1508. [CrossRef]

7.   Quddus, M.A. Crop production growth in different agro-ecological zones of Bangladesh. *J. Bangladesh Agric. Univ.* **2009**, *7*, 351–360. [CrossRef]

8.   Zappa, M.; Rotach, M.W.; Arpagaus, M.; Dorninger, M.; Hegg, C.; Montani, A.; Ranzi, R.; Ament, F.; Germann, U.; Grossi, G.; et al. MAP D-PHASE: Real-time demonstration of hydrological ensemble prediction systems. *Atmos. Sci. Lett.* **2008**, *9*, 80–87. [CrossRef]

9.   Viviroli, D.; Mittelbach, H.; Gurtz, J.; Weingartner, R. Continuous simulation for flood estimation in ungauged mesoscale catchments of Switzerland—Part II: Parameter regionalisation and flood estimation results. *J. Hydrol.* **2009**, *377*, 208–225. [CrossRef]

10.   Ahmad, Q.K.; Ahmed, A.U. Regional Cooperation in Flood Management in the Ganges-Brahmaputra-Meghna Region: Bangladesh Perspective. *Nat. Hazards* **2003**, *28*, 191–198. [CrossRef]

11.   Bakker, M.H.N. Transboundary River Floods and Institutional Capacity1. *JAWRA J. Am. Water Resour. Assoc.* **2009**, *45*, 553–566. [CrossRef]

12.   Balthrop, C.; Hossain, F. Short note: A review of state of the art on treaties in relation to management of transboundary flooding in international river basins and the Global Precipitation Measurement mission. *Water Policy* **2010**, *12*, 635–640. [CrossRef]

13.   Hay, L.E.; Clark, M.P. Use of statistically and dynamically downscaled atmospheric model output for hydrologic simulations in three mountainous basins in the western United States. *J. Hydrol.* **2003**, *282*, 56–75. [CrossRef]

14.   Ines, A.V.M.; Hansen, J.W. Bias correction of daily GCM rainfall for crop simulation studies. *Agric. For. Meteorol.* **2006**, *138*, 44–53. [CrossRef]

15.   Christensen, J.H.; Boberg, F.; Christensen, O.B.; Lucas-Picher, P. On the need for bias correction of regional climate change projections of temperature and precipitation. *Geophys. Res. Lett.* **2008**, *35*, L20709. [CrossRef]

16.   Piani, C.; Weedon, G.P.; Best, M.; Gomes, S.M.; Viterbo, P.; Hagemann, S.; Haerter, J.O. Statistical bias correction of global simulated daily precipitation and temperature for the application of hydrological models. *J. Hydrol.* **2010**, *395*, 199–215. [CrossRef]

17.   Ehret, U.; Zehe, E.; Wulfmeyer, V.; Warrach-Sagi, K.; Liebert, J. HESS Opinions "Should we apply bias correction to global and regional climate model data?". *Hydrol. Earth Syst. Sci.* **2012**, *16*, 3391–3404. [CrossRef]

18.   Teutschbein, C.; Seibert, J. Bias correction of regional climate model simulations for hydrological climate-change impact studies: Review and evaluation of different methods. *J. Hydrol.* **2012**, *456*, 12–29. [CrossRef]

19.   Chen, J.; St-Denis, B.G.; Brissette, F.P.; Lucas-Picher, P. Using Natural Variability as a Baseline to Evaluate the Performance of Bias Correction Methods in Hydrological Climate Change Impact Studies. *J. Hydrometeor.* **2016**, *17*, 2155–2174. [CrossRef]

20.   Islam, M.N.; Uyeda, H. Use of TRMM in determining the climatic characteristics of rainfall over Bangladesh. *Remote Sens. Environ.* **2007**, *108*, 264–276. [CrossRef]

21.   Nishat, B.; Rahman, S.M.M. Water Resources Modeling of the Ganges-Brahmaputra-Meghna River Basins Using Satellite Remote Sensing Data1. *JAWRA J. Am. Water Resour. Assoc.* **2009**, *45*, 1313–1327. [CrossRef]

22.   Valeriano, O.C.S.; Koike, T.; Rahman, M. Towards global river discharge assessment using a distributed hydrological model and global data sets. *Investig. Métodos J. Boliv. Priv. Univ.* **2010**, *9*, 95–102.

23.   Islam, A.S.; Haque, A.; Bala, S.K. Hydrologic characteristics of floods in Ganges–Brahmaputra–Meghna (GBM) delta. *Nat. Hazards* **2010**, *54*, 797–811. [CrossRef]

24.   Prasanna, V.; Subere, J.; Das, D.K.; Govindarajan, S.; Yasunari, T. Development of daily gridded rainfall dataset over the Ganga, Brahmaputra and Meghna river basins. *Meteorol. Appl.* **2014**, *21*, 278–293. [CrossRef]

25.   Siddique-E-Akbor, A.H.M.; Hossain, F.; Sikder, S.; Shum, C.K.; Tseng, S.; Yi, Y.; Turk, F.J.; Limaye, A. Satellite Precipitation Data–Driven Hydrological Modeling for Water Resources Management in the Ganges, Brahmaputra, and Meghna Basins. *Earth Interact.* **2014**, *18*, 1–25. [CrossRef]

26.   Shepard, D. A Two-dimensional Interpolation Function for Irregularly-spaced Data. In Proceedings of the 23rd ACM National Conference, Las Vegas, NV, USA, 27–29 August 1968; Blue, R.B., Sr., Rosenberg, A.M., Eds.; ACM Press: New York, NY, USA, 1968; pp. 517–524.

27.   Dirks, K.N.; Hay, J.E.; Stow, C.D.; Harris, D. High-resolution studies of rainfall on Norfolk Island: Part II: Interpolation of rainfall data. *J. Hydrol.* **1998**, *208*, 187–193. [CrossRef]

28.   Heistermann, M.; Kneis, D. Benchmarking quantitative precipitation estimation by conceptual rainfall-runoff modeling. *Water Resour. Res.* **2011**, *47*, W06514. [CrossRef]

29. Lehner, B.; Verdin, K.; Jarvis, A. New global hydrography derived from spaceborne elevation data. *Eos Trans. Am. Geophys. Union* **2008**, *89*, 2. [CrossRef]

30. Parry, L. Think the weather bad's here? Spare a thought for these Indian villagers who live in the wettest place in the world with 40 FEET of rain a year, Daily Mail, UK. 2013. Available online: http://www.dailymail.co.uk/news/article-2471421/Indias-Mawsynram-villagers-live-wettest-place-world-40-FEET-rain-year.html (accessed on 24 May 2018).

31. Tateishi, R.; Hoan, N.T.; Kobayashi, T.; Alsaaideh, B.; Tana, G.; Phong, D.X. Production of Global Land Cover Data—GLCNMO2008. *J. Geogr. Geol.* **2014**, *6*, 99. [CrossRef]

32. Farr, T.G.; Rosen, P.A.; Caro, E.; Crippen, R.; Duren, R.; Hensley, S.; Kobrick, M.; Paller, M.; Rodriguez, E.; Roth, L.; et al. The Shuttle Radar Topography Mission. *Rev. Geophys.* **2007**, *45*, RG2004. [CrossRef]

33. Romilly, T.G.; Gebremichael, M. Evaluation of satellite rainfall estimates over Ethiopian river basins. *Hydrol Earth Syst Sci* **2011**, *15*, 1505–1514. [CrossRef]

34. Menne, M.J.; Durre, I.; Vose, R.S.; Gleason, B.E.; Houston, T.G. An Overview of the Global Historical Climatology Network-Daily Database. *J. Atmospheric Ocean. Technol.* **2012**, *29*, 897–910. [CrossRef]

35. Funk, C.; Hoell, A.; Shukla, S.; Bladé, I.; Liebmann, B.; Roberts, J.B.; Robertson, F.R.; Husak, G. Predicting East African spring droughts using Pacific and Indian Ocean sea surface temperature indices. *Hydrol. Earth Syst. Sci.* **2014**, *18*, 4965–4978. [CrossRef]

36. Funk, C.; Peterson, P.; Landsfeld, M.; Pedreros, D.; Verdin, J.; Shukla, S.; Husak, G.; Rowland, J.; Harrison, L.; Hoell, A.; et al. The climate hazards infrared precipitation with stations—A new environmental record for monitoring extremes. *Sci. Data* **2015**, *2*, sdata201566. [CrossRef] [PubMed]

37. Kubota, T.; Shige, S.; Hashizume, H.; Aonashi, K.; Takahashi, N.; Seto, S.; Hirose, M.; Takayabu, Y.N.; Ushio, T.; Nakagawa, K.; et al. Global Precipitation Map Using Satellite-Borne Microwave Radiometers by the GSMaP Project: Production and Validation. *IEEE Trans. Geosci. Remote Sens.* **2007**, *45*, 2259–2275. [CrossRef]

38. Okamoto, K.; Takahashi, N.; Iwanami, K.; Shige, S.; Kubota, T. High precision and high resolution global precipitation map from satellite data. In Proceedings of the 2008 Microwave Radiometry and Remote Sensing of the Environment, Firenze, Italy, 11–14 March 2008; pp. 1–4.

39. Aonashi, K.; Awaka, J.; Hirose, M.; Kozu, T.; Kubota, T.; Liu, G.; Shige, S.; Kida, S.; Seto, S.; Takahashi, N.; et al. GSMaP Passive Microwave Precipitation Retrieval Algorithm: Algorithm Description and Validation. *J. Meteorol. Soc. Jpn. Ser. II* **2009**, *87A*, 119–136. [CrossRef]

40. Joyce, R.J.; Janowiak, J.E.; Arkin, P.A.; Xie, P. CMORPH: A Method that Produces Global Precipitation Estimates from Passive Microwave and Infrared Data at High Spatial and Temporal Resolution. *J. Hydrometeorol.* **2004**, *5*, 487–503. [CrossRef]

41. Ushio, T.; Sasashige, K.; Kubota, T.; Shige, S.; Okamoto, K.; Aonashi, K.; Inoue, T.; Takahashi, N.; Iguchi, T.; Kachi, M.; et al. A Kalman Filter Approach to the Global Satellite Mapping of Precipitation (GSMaP) from Combined Passive Microwave and Infrared Radiometric Data. *J. Meteorol. Soc. Jpn. Ser. II* **2009**, *87A*, 137–151. [CrossRef]

42. Seto, S.; Takahashi, N.; Iguchi, T. Rain/No-Rain Classification Methods for Microwave Radiometer Observations over Land Using Statistical Information for Brightness Temperatures under No-Rain Conditions. *J. Appl. Meteorol.* **2005**, *44*, 1243–1259. [CrossRef]

43. Takahashi, N.; Awaka, J. Introduction of a melting layer model to a rain retrieval algorithm for microwave radiometers. In Proceedings of the 2005 IEEE International Geoscience and Remote Sensing Symposium, Seoul, South Korea, 29 July 2005; Volume 5, pp. 3404–3409.

44. Ushio, T.; Tashima, T.; Kubota, T.; Kachi, M. Gauge adjusted Global Satellite Mapping of Precipitation (GSMaP_Gauge). In Proceedings of the 2014 XXXIth URSI on General Assembly and Scientific Symposium (URSI GASS), Beijing, China, 16–23 August 2014.

45. Huffman, G.J.; Bolvin, D.T.; Nelkin, E.J.; Wolff, D.B.; Adler, R.F.; Gu, G.; Hong, Y.; Bowman, K.P.; Stocker, E.F. The TRMM Multisatellite Precipitation Analysis (TMPA): Quasi-Global, Multiyear, Combined-Sensor Precipitation Estimates at Fine Scales. *J. Hydrometeorol.* **2007**, *8*, 38–55. [CrossRef]

46. Kummerow, C.; Simpson, J.; Thiele, O.; Barnes, W.; Chang, A.T.C.; Stocker, E.; Adler, R.F.; Hou, A.; Kakar, R.; Wentz, F.; et al. The Status of the Tropical Rainfall Measuring Mission (TRMM) after Two Years in Orbit. *J. Appl. Meteorol.* **2000**, *39*, 1965–1982. [CrossRef]

47.　Rudolf, B. Management and analysis of precipitation data on a routine basis, in precipitation and evaporation. In Proceedings of the International WMO/IAHS/ETH Symposium on Precipitation and Evaporation; Slovak Hydrometeorological Institute: Bratislava, Slovakia, 1993; pp. 69–76.

48.　Xie, P.; Arkin, P.A. Analyses of Global Monthly Precipitation Using Gauge Observations, Satellite Estimates, and Numerical Model Predictions. *J. Clim.* **1996**, *9*, 840–858. [CrossRef]

49.　Beck, H.E.; van Dijk, A.I.J.M.; Levizzani, V.; Schellekens, J.; Miralles, D.G.; Martens, B.; de Roo, A. MSWEP: 3-hourly 0.25° global gridded precipitation (1979–2015) by merging gauge, satellite, and reanalysis data. *Hydrol. Earth Syst. Sci.* **2017**, *21*, 589–615. [CrossRef]

50.　Beck, H.E.; Vergopolan, N.; Pan, M.; Levizzani, V.; van Dijk, A.I.J.M.; Weedon, G.P.; Brocca, L.; Pappenberger, F.; Huffman, G.J.; Wood, E.F. Global-scale evaluation of 22 precipitation datasets using gauge observations and hydrological modeling. *Hydrol. Earth Syst. Sci.* **2017**, *21*, 6201–6217. [CrossRef]

51.　Ebert, E.E.; Janowiak, J.E.; Kidd, C. Comparison of Near-Real-Time Precipitation Estimates from Satellite Observations and Numerical Models. *Bull. Am. Meteorol. Soc.* **2007**, *88*, 47–64. [CrossRef]

52.　Wang, J.; Hong, Y.; Li, L.; Gourley, J.J.; Khan, S.I.; Yilmaz, K.K.; Adler, R.F.; Policelli, F.S.; Habib, S.; Irwn, D.; et al. The coupled routing and excess storage (CREST) distributed hydrological model. *Hydrol. Sci. J.* **2011**, *56*, 84–98. [CrossRef]

53.　Jiang, S.; Ren, L.; Hong, Y.; Yong, B.; Yang, X.; Yuan, F.; Ma, M. Comprehensive evaluation of multi-satellite precipitation products with a dense rain gauge network and optimally merging their simulated hydrological flows using the Bayesian model averaging method. *J. Hydrol.* **2012**, *452–453*, 213–225. [CrossRef]

54.　Yong, B.; Hong, Y.; Ren, L.-L.; Gourley, J.J.; Huffman, G.J.; Chen, X.; Wang, W.; Khan, S.I. Assessment of evolving TRMM-based multisatellite real-time precipitation estimation methods and their impacts on hydrologic prediction in a high latitude basin. *J. Geophys. Res. Atmos.* **2012**, *117*, D09108. [CrossRef]

55.　Haile, A.T.; Habib, E.; Rientjes, T.H.M. Evaluation of the climate prediction center CPC morphing technique CMORPH rainfall product on hourly time scales over the source of the Blue Nile river. *Hydrol. Process.* **2013**, *27*, 1829–1938. [CrossRef]

56.　Guo, H.; Chen, S.; Bao, A.; Hu, J.; Gebregiorgis, A.S.; Xue, X.; Zhang, X. Inter-Comparison of High-Resolution Satellite Precipitation Products over Central Asia. *Remote Sens.* **2015**, *7*, 7181–7211. [CrossRef]

57.　Salio, P.; Hobouchian, M.P.; García Skabar, Y.; Vila, D. Evaluation of high-resolution satellite precipitation estimates over southern South America using a dense rain gauge network. *Atmos. Res.* **2015**, *163*, 146–161. [CrossRef]

58.　Qi, W.; Zhang, C.; Fu, G.; Sweetapple, C.; Zhou, H. Evaluation of global fine-resolution precipitation products and their uncertainty quantification in ensemble discharge simulations. *Hydrol. Earth Syst. Sci.* **2016**, *20*, 903–920. [CrossRef]

59.　Su, F.; Hong, Y.; Lettenmaier, D.P. Evaluation of TRMM Multisatellite Precipitation Analysis (TMPA) and Its Utility in Hydrologic Prediction in the La Plata Basin. *J. Hydrometeorol.* **2008**, *9*, 622–640. [CrossRef]

60.　Hay, L.E.; Wilby, R.L.; Leavesley, G.H. A Comparison of Delta Change and Downscaled Gcm Scenarios for Three Mountainous Basins in the United States1. *JAWRA J. Am. Water Resour. Assoc.* **2000**, *36*, 387–397. [CrossRef]

61.　Lenderink, G.; Buishand, A.; van Deursen, W. Estimates of future discharges of the river Rhine using two scenario methodologies: Direct versus delta approach. *Hydrol. Earth Syst. Sci.* **2007**, *11*, 1145–1159. [CrossRef]

62.　Lafon, T.; Dadson, S.; Buys, G.; Prudhomme, C. Bias correction of daily precipitation simulated by a regional climate model: A comparison of methods. *Int. J. Climatol.* **2013**, *33*, 1367–1381. [CrossRef]

63.　Arias-Hidalgo, M.; Bhattacharya, B.; Mynett, A.E.; van Griensven, A. Experiences in using the TMPA-3B42R satellite data to complement rain gauge measurements in the Ecuadorian coastal foothills. *Hydrol. Earth Syst. Sci.* **2013**, *17*, 2905–2915. [CrossRef]

64.　Fang, G.H.; Yang, J.; Chen, Y.N.; Zammit, C. Comparing bias correction methods in downscaling meteorological variables for a hydrologic impact study in an arid area in China. *Hydrol. Earth Syst. Sci.* **2015**, *19*, 2547–2559. [CrossRef]

65.　Habib, E.; Haile, A.T.; Sazib, N.; Zhang, Y.; Rientjes, T. Effect of Bias Correction of Satellite-Rainfall Estimates on Runoff Simulations at the Source of the Upper Blue Nile. *Remote Sens.* **2014**, *6*, 6688–6708. [CrossRef]

66.　Bhatti, H.A.; Rientjes, T.; Haile, A.T.; Habib, E.; Verhoef, W. Evaluation of Bias Correction Method for Satellite-Based Rainfall Data. *Sensors* **2016**, *16*, 884. [CrossRef] [PubMed]

67.　Vila, D.A.; de Goncalves, L.G.G.; Toll, D.L.; Rozante, J.R. Statistical Evaluation of Combined Daily Gauge Observations and Rainfall Satellite Estimates over Continental South America. *J. Hydrometeorol.* **2009**, *10*, 533–543. [CrossRef]

68. Themeßl, M.J.; Gobiet, A.; Leuprecht, A. Empirical-statistical downscaling and error correction of daily precipitation from regional climate models. *Int. J. Climatol.* **2011**, *31*, 1530–1544. [CrossRef]

69. Sun, F.; Roderick, M.L.; Lim, W.H.; Farquhar, G.D. Hydroclimatic projections for the Murray-Darling Basin based on an ensemble derived from Intergovernmental Panel on Climate Change AR4 climate models. *Water Resour. Res.* **2011**, *47*, W00G02. [CrossRef]

70. Themeßl, M.J.; Gobiet, A.; Heinrich, G. Empirical-statistical downscaling and error correction of regional climate models and its impact on the climate change signal. *Clim. Chang.* **2012**, *112*, 449–468. [CrossRef]

71. Chen, J.; Brissette, F.P.; Chaumont, D.; Braun, M. Finding appropriate bias correction methods in downscaling precipitation for hydrologic impact studies over North America. *Water Resour. Res.* **2013**, *49*, 4187–4205. [CrossRef]

72. Wilcke, R.A.I.; Mendlik, T.; Gobiet, A. Multi-variable error correction of regional climate models. *Clim. Chang.* **2013**, *120*, 871–887. [CrossRef]

73. Wood, A.W.; Leung, L.R.; Sridhar, V.; Lettenmaier, D.P. Hydrologic Implications of Dynamical and Statistical Approaches to Downscaling Climate Model Outputs. *Clim. Chang.* **2004**, *62*, 189–216. [CrossRef]

74. Hasan, M.M.; Sharma, A.; Johnson, F.; Mariethoz, G.; Seed, A. Merging radar and in situ rainfall measurements: An assessment of different combination algorithms. *Water Resour. Res.* **2016**, *52*, 8384–8398. [CrossRef]

75. Stock, J.; Watson, M. A Comparison of Linear and Nonlinear Univariate Models for Forecasting Macroeconomic Time Series. In *Cointegration, Causality and Forecasting: A Festschrift for Clive, W.J. Granger*; Engle, R., White, H., Eds.; Oxford University Press: Oxford, UK, 1999; pp. 1–44.

76. Stock, J.H.; Watson, M.W. How Did Leading Indicator Forecasts Perform during the 2001 Recession? *Econ. Q. Fed. Res. Bank Richmond* **2003**, *89*, 71–90.

77. Stock, J.H.; Watson, M.W. Combination forecasts of output growth in a seven-country data set. *J. Forecast.* **2004**, *23*, 405–430. [CrossRef]

78. Woldemeskel, F.M.; Sivakumar, B.; Sharma, A. Merging gauge and satellite rainfall with specification of associated uncertainty across Australia. *J. Hydrol.* **2013**, *499*, 167–176. [CrossRef]

79. Shen, Y.; Xiong, A.; Hong, Y.; Yu, J.; Pan, Y.; Chen, Z.; Saharia, M. Uncertainty analysis of five satellite-based precipitation products and evaluation of three optimally merged multi-algorithm products over the Tibetan Plateau. *Int. J. Remote Sens.* **2014**, *35*, 6843–6858. [CrossRef]

80. Taylor, K.E. Summarizing multiple aspects of model performance in a single diagram. *J. Geophys. Res. Atmos.* **2001**, *106*, 7183–7192. [CrossRef]

81. Sayama, T.; Ozawa, G.; Kawakami, T.; Nabesaka, S.; Fukami, K. Rainfall–runoff–inundation analysis of the 2010 Pakistan flood in the Kabul River basin. *Hydrol. Sci. J.* **2012**, *57*, 298–312. [CrossRef]

82. Sayama, T.; Tatebe, Y.; Tanaka, S. An emergency response-type rainfall-runoff-inundation simulation for 2011 Thailand floods. *J. Flood Risk Manag.* **2015**, *10*, 65–78. [CrossRef]

83. Sayama, T.; Tatebe, Y.; Iwami, Y.; Tanaka, S. Hydrologic sensitivity of flood runoff and inundation: 2011 Thailand floods in the Chao Phraya River basin. *Nat. Hazards Earth Syst. Sci.* **2015**, *15*, 1617–1630. [CrossRef]